

# Distributed Task Allocation for Multi-Agent Systems: A Submodular Optimization Approach

Jing Liu, Fangfei Li, *Member, IEEE*, Xin Jin, Yang Tang, *Fellow, IEEE*

**Abstract**—This paper investigates dynamic task allocation for multi-agent systems (MASs) under resource constraints, with a focus on maximizing the global utility of agents while ensuring a conflict-free allocation of targets. We present a more adaptable submodular maximization framework for the MAS task allocation under resource constraints. Our proposed distributed greedy bundles algorithm (DGBA) is specifically designed to address communication limitations in MASs and provides rigorous approximation guarantees for submodular maximization under  $q$ -independent systems, with low computational complexity. Specifically, DGBA can generate a feasible task allocation policy within polynomial time complexity, significantly reducing space complexity compared to existing methods. To demonstrate practical viability of our approach, we apply DGBA to the scenario of active observation information acquisition within a micro-satellite constellation, transforming the NP-hard task allocation problem into a tractable submodular maximization problem under a  $q$ -independent system constraint. Our method not only provides a specific performance bound but also surpasses benchmark algorithms in metrics such as utility, cost, communication time, and running time.

**Index Terms**—Multi-agent systems, task allocation, submodular optimization, distributed algorithms.

## I. INTRODUCTION

MULTI-AGENT task allocation is a crucial concern in a variety of real-world scenarios, including persistent surveillance [1], area exploration [2], and job automation [3]. The overarching goal is to allocate tasks to agents in an optimal or near-optimal fashion. However, this problem is universally recognized as NP-hard, posing significant difficulties

This work is supported by the National Natural Science Foundation of China under Grants 62233005, 62293502, 62173142, the Programme of Introducing Talents of Discipline to Universities (the 111 Project) under Grant B17017, in part by the Shanghai Sailing Program under Grant 23YF1409600, in part by the Young Elite Scientist Sponsorship Program by Cast under Grant YESS20220198, in part by the Fundamental Research Funds for the Central Universities, and the National Key Laboratory of Space Intelligent Control under Grant No. HTKJ2024KL502004.

Jing Liu is with the School of Mathematics, East China University of Science and Technology, Shanghai 200237, China (e-mail: y20220091@mail.ecust.edu.cn).

Fangfei Li is with the School of Mathematics and the Key Laboratory of Smart Manufacturing in Energy Chemical Process, Ministry of Education, East China University of Science and Technology, Shanghai 200237, China (e-mail: li.fangfei@163.com, lifangfei@ecust.edu.cn).

Xin Jin is with the Research Institute of Intelligent Complex Systems, Fudan University, Shanghai 200433, China, and with the Key Laboratory of Smart Manufacturing in Energy Chemical Process, Ministry of Education, East China University of Science and Technology, Shanghai 200237, China (email: jx.9810@163.com).

Yang Tang is with the Key Laboratory of Smart Manufacturing in Energy Chemical Process, Ministry of Education, East China University of Science and Technology, Shanghai, 200237, China (email: yangtang@ecust.edu.cn).

Corresponding authors: Fangfei Li and Yang Tang.

in finding optimal solutions [4], [5]. To address this challenge, researchers have developed formal mathematical models and classification frameworks for multi-agent task allocation, drawing from economics, optimization, and operations research [6]–[8].

Existing methods for task allocation in multi-agent systems (MASs) are typically categorized into centralized and distributed approaches [9], [10]. Centralized methods, such as the sequential greedy algorithm (SGA) [11], rely on a central coordinator with full access to global information to manage task assignments [12]. While capable of yielding globally optimal solutions, these methods demand substantial communication bandwidth and incur high maintenance costs for the central coordinator. In contrast, distributed algorithms have been proposed to minimize reliance on a central coordinator, thereby enhancing system robustness and real-time capabilities through parallel processing, particularly beneficial in highly dynamic environments [13]–[17].

Auction-based methods have emerged as a prevalent class of distributed task allocation algorithms, attracting significant research attention. Early contributions in this domain include the consensus-based auction algorithm (CBAA) and the consensus-based bundle algorithm (CBBA), both proposed for coordinating multiple autonomous vehicles [18]. Addressing dynamic task allocation scenarios, the greedy coalition auction algorithm (GCAA) was designed to tackle single-task allocation in spatially distributed MASs, considering both rewards and costs associated with task completion [19]. Further advancements in CBBA-based algorithms were made by [12] with the distributed matching-by-clone Hungarian-based algorithm (DM-CHBA), which addresses task allocation in MASs and handles the NP-hardness of communication. However, while these methods provide feasible solutions with a certain convergence rate, they lack a guarantee for the quality of the solutions, presenting theoretical challenges in achieving optimality [20]–[23].

Submodular optimization has been recognized as a discrete optimization method with favorable theoretical properties, widely applicable to a diverse array of combinatorial optimization problems such as weapon-target assignment, weighted coverage, entropy, and mutual information functions [24]–[29]. In [25], the authors investigated the multi-agent task allocation problem by formulating it as a matroid-constrained submodular maximization problem. They proposed a distributed greedy algorithm (DGA) to improve the efficiency of location-allocation of a constellation of Earth-observing satellites, leveraging local information and communication [24]. When

the utility functions are non-decreasing and submodular, the proposed DGA guarantees a solution with performance at least 1/2 of the optimal solution. Furthermore, the problems of robust submodular maximization under cardinality and matroid constraints were explored in [8]. In this work, the authors proposed two improved greedy algorithms, demonstrating their capability to attain provable performance bounds within the defined constraints. Moreover, the development of a distributed SGA for addressing multi-agent covering problems in an environment with obstacles was highlighted in the research by [26]. This SGA offers a more refined performance bound by delving into the curvature characteristics of submodularity.

Despite these advancements, existing approaches to task allocation reveal limitations that necessitate further investigation. Firstly, an ideal mathematical theoretical framework for optimal task allocation, particularly in scenarios with high spatiotemporal dynamics, remains absent [30]. While submodular optimization has been employed for its analytical advantages in discrete combinatorial optimization, the focus has been primarily on submodular maximization under cardinality and matroid constraints [8]. These constraints are rigid and may not be readily adaptable to the practical demands of dynamic task scheduling. The use of  $q$ -independent systems, which relax the requirements for independent sets, offers a more natural formulation of the submodular maximization problem for addressing dynamic task allocation under resource constraints. Nevertheless, research on dynamic task allocation under  $q$ -independent system constraints remains relatively limited. Additionally, there are limited studies to address dynamic task allocation in a purely distributed manner, with task allocation algorithms providing approximate guarantees for static task allocation problems under cardinality and matroid constraints. However, the theoretical analyses of these algorithms may not hold up when applied to various constraints such as limited fuel costs for agents and real-time communication constraints [31]–[33]. Finally, due to the high spatiotemporal dynamics of the distribution of agents and targets, considering multiple constraints, including agent and target dynamics, cost limitations, and the necessity for conflict-free allocations, the MAS task allocation as an Integer Nonlinear Programming (INP) problem is NP-hard. This complexity necessitates exponential time to achieve optimal solutions, thereby hindering the rapid development of effective conflict-free task allocation [18], [25].

Motivated by these challenges, this paper focuses on dynamic task allocation for MASs under resource constraints using submodular optimization. The objective is to achieve a conflict-free task allocation policy, maximizing the global utility of the MAS. We present a submodular maximization framework and a distributed greedy bundles algorithm (DGBA), which strike a significant balance between theoretical performance and computational efficiency, thereby facilitating a more equitable distribution of resources in dynamic settings. The primary contributions are outlined as follows:

- 1) *Extensive Adaptability*: We develop a more comprehensive submodular maximization framework for MASs task allocation under resource constraints (referred to Problem 1). This framework extends existing models

by integrating  $q$ -independent systems, offering a more flexible alternative to cardinality and matroid constraints [8], [29]. Through rigorous proofs and analysis, we establish the theoretical performance guarantees of DGBA (Theorem 1 and Theorem 2), without requiring the augmentation property of matroids.

- 2) *Low Computational Complexity*: The proposed DGBA employs local greedy techniques for distributed decision-making and a negotiated consensus mechanism to ensure conflict-free task allocation. By focusing on the information of task bundles, DGBA enhances computational efficiency. A comprehensive analysis of computational complexity (Theorem 3) reveals that DGBA can generate a feasible allocation policy within polynomial time complexity of  $O(N^2 + NM)$ , and it exhibits a lower space complexity of  $O(N^2 + M)$  than traditional methods such as CBBA [18] and DGA [25], especially when the number of tasks surpasses the agents.
- 3) *Tractable NP-Hard Problem*: We tackle the NP-hard active observation information acquisition application by transforming it into a manageable submodular maximization problem under  $q$ -independent system constraints (referred to as Problem 2). By establishing a utility function for the submodular structure (Theorem 4), we derive a concrete performance bound (Theorem 5). Simulation studies indicate that DGBA's global utility surpasses that of the benchmark CBBA method by over 60%. With effective control of total cost, DGBA reduces communication time per iteration by 0.05 seconds and overall running time by 10 seconds, outperforming other selected algorithms, such as CBBA [18] and DGA [25].

The remainder of this paper is structured as follows. In Section II, we formulate the optimal task allocation problems. Section III presents the DGBA, which is central to our approach. Section IV then offers a thorough analysis of the performance guarantees associated with the DGBA. Section V provides a specific application and numerical simulations to demonstrate the effectiveness and feasibility of our approach. Finally, Section VI concludes the paper. Additionally, Appendix A introduces key concepts of submodular set functions, Appendix B provides the performance analysis of DGBA regarding the application, and Appendix C contains proofs of all lemmas and theorems in this paper.

*Notations*: In this paper, we assume that all the matrices have appropriate dimensions.  $\mathbb{Z}_+$  and  $\mathbb{Z}$  represent the set of positive integers and the set of integers.  $\mathbb{R}_+$ ,  $\mathbb{R}$ ,  $\mathbb{R}^N$ , and  $\mathbb{R}^{N \times N}$  are the set of positive real numbers, the set of real numbers, the  $N$ -dimensional real vectors, and the  $N \times N$ -dimensional real matrices, respectively. For any set  $A$ ,  $2^A$  represents its power set, and  $|A|$  represents the cardinality of  $A$ . If  $B$  is another set,  $A \setminus B$  is the set of elements belonging to  $A$  but not to  $B$ .  $\|\cdot\|$  refers to Euclidean norm. Lastly, the ceiling function is defined as  $\lceil x \rceil = \min\{n \in \mathbb{Z} \mid n \geq x\}$ .

## II. TASK ALLOCATION PROBLEMS

In this section, we provide a submodular maximization framework and outline the definitions and assumptions for task

allocation problems in MASs. Additional concepts, including the definitions of submodularity and independent systems, are provided in Appendix A.

### A. Problem Framework

This study focuses on a MAS comprised of  $N$  agents assigned to execute a finite set of  $M$  targets within a spatial environment. The agents are indexed by the set  $\mathcal{I} = \{1, \dots, N\}$ , while the targets are indexed by  $\mathcal{J} = \{1, \dots, M\}$ . For each target  $j \in \mathcal{J}$ , an expected end time for a time window is designated as  $t_{e,j}$ , and the expected duration for the execution is represented as  $\tau_j^{obs}$ . The entire time interval  $[0, t_{e,j}]$  is discretized into  $T$  equally spaced time intervals, each represented by  $\tau$ .

For each agent  $i \in \mathcal{I}$  at time step  $t$ , let the state and control input be denoted by  $\mathbf{x}_i(t) \in \mathbb{R}^{n_{\mathbf{x}_i(t)}}$  and  $\mathbf{u}_i(t) \in \mathbb{R}^{n_{\mathbf{u}_i(t)}}$ , respectively.

- **Agent Dynamics:** We consider a scenario where each agent  $i \in \mathcal{I}$ , equipped with a sensor, follows a noiseless, nonlinear, and continuous agent dynamic:

$$\dot{\mathbf{x}}_i(t) = \mathcal{F}_i(\mathbf{x}(t), \mathbf{u}(t)), \forall i \in \mathcal{I}, \quad (1)$$

where  $\mathcal{F}_i(\cdot)$  represents the dynamic model of agent  $i$ ,  $\mathbf{x}(t) = \{\mathbf{x}_i(t) \mid \forall i \in \mathcal{I}\}$  denotes the joint state of the MAS, and  $\mathbf{u}(t) = \{\mathbf{u}_i(t) \mid \forall i \in \mathcal{I}\}$  signifies the joint control input at time step  $t$ .

- **Target Dynamics:** The dynamic of each target  $j \in \mathcal{J}$  is assumed to follow:

$$\dot{\mathbf{y}}_j(t) = \mathcal{H}_j(\mathbf{y}_j(t)) + \eta_j(t), \forall j \in \mathcal{J}, \quad (2)$$

where  $\mathcal{H}_j(\cdot)$  is the dynamic model of target  $j$ ,  $\eta_j(t)$  represents a drag force proportional to the target's velocity  $\mathbf{w}_j(t)$ , given by  $\eta_j(t) = -k_d \mathbf{w}_j(t)$ , where  $k_d \in \mathbb{R}_+$  is a constant reflecting the environmental density. Denote  $\mathbf{y}(t) = \{\mathbf{y}_j(t) \mid \forall j \in \mathcal{J}\}$  as the joint state of targets at time step  $t$ .

- **Communication Network:** Define  $\mathcal{G}(t) = (\mathcal{I}, \mathcal{E}(t))$  as the undirected graph representing the communication network at time step  $t$ , where  $\mathcal{I}$  is the agent set, and  $\mathcal{E}(t) \subseteq \mathcal{I} \times \mathcal{I}$  is the set of edges. The existence of an edge  $(i', i) \in \mathcal{E}(t)$  signifies that a communication link between agents  $i'$  and  $i$  at time step  $t$ . An adjacency matrix corresponding to the communication network  $\mathcal{G}(t)$  is given by  $\mathcal{A}(t) = [a_{ii'}(t)] \in \mathbb{R}^{N \times N}$ , where  $a_{ii'}(t) > 0$  if  $(i', i) \in \mathcal{E}(t)$  and  $i' \neq i$ ; otherwise,  $a_{ii'}(t) = 0$ . The neighbor set of agent  $i$  at time step  $t$  is represented as  $\mathcal{N}_i(t) = \{i' \in \mathcal{I} \mid a_{ii'}(t) > 0\}$ .
- **Constraints:** Each agent  $i \in \mathcal{I}$  continuously moves toward its assigned target within the time interval  $[0, t_{e,j}]$ , and performs the task in a conflict-free manner. We assume that the allocation complies with  $q$ -independent system constraints, denoted as  $\Pi(t) \in \mathcal{S}_q$ . Here,  $(\Omega, \mathcal{S}_q)$  represents a  $q$ -independent system, where  $\Omega = \mathcal{I} \times \mathcal{J}$  denotes the finite ground set, and  $\mathcal{S}_q$  contains all currently feasible allocation policies that satisfy  $q$ -independent system constraints.

- **Objective:** The primary objective for the MAS is the joint optimization of the allocation policy  $\Pi(t)$ , which assigns mobile agents to targets while satisfying the given constraints. This process aims to maximize the task allocation utility  $\mathcal{O}(\cdot)$  for the  $M$  targets of interest at each discrete time step  $t$ . The objective function is formulated as

$$\mathcal{O}(\Pi(t) \mid \mathbf{x}(t), \mathbf{y}(t)), \quad (3)$$

where the policy  $\Pi(t) \subseteq \Omega$ , with each element  $\pi = (i, j) \in \Pi(t)$  indicates that agent  $i$  is allocated to target  $j$  at time step  $t$ . In this paper, we focus on an objective function (3) that is normalized, non-decreasing, and submodular. For instance, in environment monitoring applications,  $\mathcal{O}(\cdot)$  may represent the collective coverage area provided by a network of sensors [11]. In target tracking scenarios,  $\mathcal{O}(\cdot)$  could be constructed using the cumulative Kalman filtering error estimated by the sensors [34]. For simplicity,  $\mathcal{O}(\Pi(t))$  is used to represent the objective function  $\mathcal{O}(\Pi(t) \mid \mathbf{x}(t), \mathbf{y}(t))$  in subsequent discussions.

*Remark 1:* The agents under consideration are equipped with propulsion systems capable of overcoming or compensating for encountered resistance. Consequently, the agents are modeled to operate autonomously within the environment, largely unaffected by external forces, such as air resistance [35]. On the contrary, the including a drag force  $\eta_j(t)$  in the dynamics of targets (2) serves to simulate the resistive forces encountered by targets as they move through the environment. The drag force  $\eta_j(t)$  is typically assumed to be proportional to the target's velocity, reflecting real-world physical phenomena [36].

*Remark 2:* The  $q$ -independent system can be defined as a model for task allocation under resource constraints, where the parameter  $q$  imposes the upper bound on the ratio of sizes between any two allocation sets. It can characterize the nature of the task, resource demands, and time constraints, thereby facilitating a fair and efficient distribution of tasks among agents. This concept finds application in various problems within the domain of MASs, such as resource allocation, task scheduling, and network design. For instance, in sensor networks,  $q$ -independent systems can model capability constraints of agents, where each sensor can monitor a finite number of targets with minimum overlap [37].

### B. Problem Definitions and Assumptions

In addressing the dynamic task allocation problems among mobile agents and targets, we aim to assign agents to targets in a conflict-free manner, thereby maximizing the objective function  $\mathcal{O}(\Pi(t))$  for given sets of  $N$  agents and  $M$  targets at each discrete time step  $t$ . We present the following optimization problem:

*Problem 1:* Let a finite ground set  $\Omega$  and a normalized, non-decreasing, and submodular function  $\mathcal{O}(\cdot)$ , the goal is to maximize  $\mathcal{O}(\Pi(t))$  over the set  $\Pi(t)$  at each time step  $t$  while adhering to the  $q$ -independent system constraint  $\Pi(t) \in \mathcal{S}_q$ . We investigate the following submodular maximization

problem with a  $q$ -independent system constraint:

$$\max_{\Pi(t) \subseteq \Omega} \mathcal{O}(\Pi(t)) = \sum_{j=1}^M \mathcal{O}_j(\Pi(t)) \quad (4a)$$

$$s.t. \quad \Pi(t) \in \mathcal{S}_q, \quad (4b)$$

where  $(\Omega, \mathcal{S}_q)$  forms a  $q$ -independent system. The utility function for target  $j$  is denoted by  $\mathcal{O}_j(\cdot)$ , which is presumed to be normalized, non-decreasing, and submodular.

We denote  $\mathcal{J}_i(\Omega)$  as the set of targets that agent  $i$  can select from. The assumptions of the dynamic task allocation problem are outlined as follows:

*Assumption 1:* Each agent within the MAS is equipped with specific information and communication capabilities, outlined as follows:

- *Initial global information:* The MAS operates on a centralized planning platform, which possesses prior knowledge of the initial positions and velocities of targets. This information is utilized for task evaluation and assignment procedures.
- *Local information:* Each agent  $i \in \mathcal{I}$  possesses real-time knowledge of the joint state  $\mathbf{y}(t)$  of targets, and can evaluate the utility function  $\mathcal{O}_j(\cdot)$  that falls within its feasible targets set  $\mathcal{J}_i(\Omega)$ .
- *Limited communication:* Each agent  $i \in \mathcal{I}$  operates within a finite communication range  $R_i^c$ .

*Assumption 2 ([38]):* Tasks are regarded as indivisible meta-tasks, meaning that once an agent initiates engagement with a target, the execution process cannot be interrupted or preempted.

*Remark 3:* Given the finite communication range  $R_i^c$ , agent  $i$  is restricted to exchanging information only with its neighboring agents  $\mathcal{N}_i(t)$  at time step  $t$ . The process of reaching a consensus on MAS attributes across the entire network may require multiple iterative exchanges.

### III. A DISTRIBUTED GREEDY ALGORITHM FOR DYNAMIC TASK ALLOCATION

To tackle the submodular maximization problem outlined in Problem 1, we propose the distributed solution, where each agent makes decisions based on local information and limited communication. Our approach, the distributed greedy bundles algorithm (DGBA), capitalizes the advantageous properties of the utility function  $\mathcal{O}(\Pi(t))$ , as detailed in Section IV. The main pseudocode is presented in Algorithm 1, which encompasses three distinct phases, each detailed through separate algorithms: Algorithm 2, Algorithm 3, and Algorithm 4.

#### A. Distributed Greedy Bundles Algorithm

This proposed DGBA focuses on the efficient construction of task bundles. It is a distributed task allocation algorithm that capitalizes on the efficiency of greedy approaches to achieve rapid convergence to a feasible solution. Let  $\mathcal{J}_i(t+1)$  represent the index set of targets that have not been allocated at time step  $t+1$ . Additionally, we define  $\delta_{(i,j)}(\Pi(t))$  as the marginal utility introduced by an element  $(i,j)$  into the allocation  $\Pi(t)$ , which is formulated as  $\delta_{(i,j)}(\Pi(t)) = \mathcal{O}_j(\Pi(t) \cup \{(i,j)\}) - \mathcal{O}_j(\Pi(t))$ .

---

#### Algorithm 1 Distributed Greedy Bundles Algorithm (DGBA)

---

**Input:**  $\mathcal{I}, \mathcal{J}, \mathbf{x}(0), \mathbf{y}(0), \mathcal{A}(0), T$ .

**Output:** Task allocation policy  $\Pi(T)$

- 1: **for** iteration  $t = 0, 1, \dots, T - 1$  **do**
  - 2:   **for** each agent  $i \in \mathcal{I}$  **do**
  - // Phase I: Assignment, described in Algorithm 2 //
  - 3:     ASSIGNMENTPHASE( $\mathbf{W}_i, \mathbf{B}_i, \mathbf{F}_i, \mathbf{x}_i(t), \mathbf{y}(t)$ ).
  - // Phase II: Communication, described in Algorithm 3 //
  - 4:     COMMUNICATEPHASE( $\mathbf{W}_i, \mathbf{B}_i, \mathbf{F}_i, \mathcal{A}(t)$ ).
  - // Phase III: Implementation and Update, described in Algorithm 4 //
  - 5:     IMPLEUPATEPHASE( $\mathbf{W}_i, \mathbf{x}_i(t), \mathbf{y}(t)$ ).
  - 6:   **end for**
  - 7:   Update  $\mathcal{A}(t+1)$  based on  $\mathbf{x}(t+1)$ .
  - 8: **end for**
- 

Each agent in the MAS maintains three distinct task bundles, which are iteratively updated at each time step.

- 1) **Allocation Bundle  $\mathbf{W}_i$ :** A vector of length  $N$  representing agent  $i$ 's knowledge regarding task allocation across all agents, with  $\mathbf{W}_i \in \{0, 1, \dots, M\}^N$ . Specifically,  $\mathbf{W}_i$  encompasses the targets selected from the target set  $\mathcal{J}$  of  $N$  agents. The  $i'$ -th element of  $\mathbf{W}_i \in \{0, 1, \dots, M\}$ , denoted as  $\mathbf{W}_{i,i'}$ , indicates the target index allocated to agent  $i'$  as perceived by agent  $i$  at each time step.
- 2) **Utility Bundle  $\mathbf{B}_i$ :** A vector of length  $N$  that captures the marginal utility perceived by agent  $i$  associated with the task allocation  $\Pi(t)$ . Specifically, the  $i'$ -th element of  $\mathbf{B}_i$ , denoted as  $\mathbf{B}_{i,i'} = \delta_{(i,\hat{j}_i)}(\Pi(t))$ , quantifies the expected individual utility that agent  $i'$  would derive from executing the task  $\mathbf{W}_{i,i'}$ . The utility bundle for agent  $i$  is updated as  $\mathbf{B}_i = \{\mathbf{B}_{i,1}^-, \dots, \mathbf{B}_{i,i-1}^-, \delta_{(i,\hat{j}_i)}(\Pi(t)), \mathbf{B}_{i,i+1}^-, \dots, \mathbf{B}_{i,N}^-\}^\top$ , where  $\mathbf{B}_{i,i'}^-$  refers to the element from the previous iteration's utility bundle  $\mathbf{B}_i^-$ .
- 3) **Finalization Bundle  $\mathbf{F}_i$ :** A vector of length  $N$  indicating the finalized task allocations of all agents, denoted as  $\mathbf{F}_i \in \{0, 1\}^N$ . Specifically, the  $i'$ -th element of  $\mathbf{F}_i$  is set to 1 if agent  $i'$  intends to maintain their current task allocation; otherwise,  $\mathbf{F}_{i,i'} = 0$ . This vector aids in excluding agents with completed allocations from further assignment processes.

The DGBA methodology, as outlined in Algorithm 1, comprises three main phases: the assignment phase (Algorithm 2), the communication phase (Algorithm 3), the implementation and update phase (Algorithm 4). We now describe each stage in detail.

#### B. Phase I: Assignment

The initial phase of DGBA involves a greedy assignment process, as outlined in Algorithm 2. If agent  $i$  remains without an assigned task (line 4), the algorithm proceeds as follows: Initially, the allocation policy  $\Pi(t)$  from the preceding time step is retrieved (line 5). Subsequently, the agent identifies the target  $\hat{j}_i$  from the set of available targets  $\mathcal{J}_i(t+1)$  with the objective of maximizing the expected marginal utility

**Algorithm 2** Select an Unassigned Task for Agent  $i$ 


---

```

1: function ASSIGNMENTPHASE( $\mathbf{W}_i, \mathbf{B}_i, \mathbf{F}_i, \mathbf{x}_i(t), \mathbf{y}(t)$ )
2: Input:  $\mathbf{W}_i, \mathbf{B}_i, \mathbf{F}_i, \mathbf{x}_i(t), \mathbf{y}(t)$ 
3: Output:  $\mathbf{W}_i, \mathbf{B}_i, \mathbf{F}_i$ 
4:   if  $\mathbf{F}_{i,i} = 0$  then
5:      $\Pi(t) \leftarrow \mathbf{W}_i$ .
6:     for  $j \in \mathcal{J}_i(t+1)$  do
7:        $\delta_{(i,j)}(\Pi(t)) \leftarrow \mathcal{O}_j(\Pi(t) \cup \{(i,j)\}) - \mathcal{O}_j(\Pi(t))$ .
8:     end for
9:      $\hat{j}_i \leftarrow \arg \max_{j \in \mathcal{J}_i(t+1)} \delta_{(i,j)}(\Pi(t))$ .
10:     $\mathbf{W}_{i,i} \leftarrow \hat{j}_i$ .
11:     $\mathbf{B}_{i,i} \leftarrow \delta_{(i,\hat{j}_i)}(\Pi(t))$ .
12:     $\mathbf{F}_{i,i} \leftarrow \mathbf{F}_{i,i}$ .
13:  end if
14:  if  $\sum_{i'=1}^N \mathbf{F}_{i,i'} = N$  then
15:    Terminate.
16:  end if
17: end function

```

---

**Algorithm 3** Communicate the Bundles to Conflict Resolution

---

```

1: function COMMUCATEPHASE( $\mathbf{W}_i, \mathbf{B}_i, \mathbf{F}_i, \mathcal{A}(t)$ )
2: Input:  $\mathbf{W}_i, \mathbf{B}_i, \mathbf{F}_i, \mathcal{A}(t)$ 
3: Output:  $\mathbf{W}_i, \mathbf{B}_i, \mathbf{F}_i$ 
4:   for  $i' \in \mathcal{N}_i(t)$  do
5:      $\mathbf{W}_{i,i'} \leftarrow \mathbf{W}_{i',i'}$ .
6:      $\mathbf{B}_{i,i'} \leftarrow \mathbf{B}_{i',i'}$ .
7:      $\mathbf{F}_{i,i'} \leftarrow \mathbf{F}_{i',i'}$ .
8:   end for
9:    $\mathcal{K}_i \leftarrow \{i' \mid \mathbf{W}_{i,i'} = \mathbf{W}_{i,i}, \mathbf{F}_{i,i'} = 0\}$ .
10:   $\hat{i} \leftarrow \arg \max_{i \in \mathcal{K}_i} \mathbf{B}_{i,i'}$ .
11:   $\mathbf{F}_{i,\hat{i}} = 1$ .
12:  for  $i \in \mathcal{K}_i \setminus \hat{i}$  do
13:     $\mathbf{W}_{i,i'} = 0$ .
14:     $\mathbf{B}_{i,i'} = 0$ .
15:  end for
16: end function

```

---

$\delta_{(i,j)}(\Pi(t))$  (lines 6-9). Agent  $i$  then updates the element  $\mathbf{W}_{i,i}$  of the allocation bundle  $\mathbf{W}_i$ , the element  $\mathbf{B}_{i,i}$  of the utility bundle  $\mathbf{B}_i$ , and the element  $\mathbf{F}_{i,i}$  of the finalization bundle  $\mathbf{F}_i$  with the selected target (lines 10-12). Moreover, if every element within the bundle  $\mathbf{F}_i$  is 1, indicating that all agents have finalized their task allocations, the assignment process for the current time step is terminated (lines 14-16).

**C. Phase II: Communication**

The communication phase of DGBA, as outlined in Algorithm 3, involves an exchange of information among agents. Specifically, each agent  $i \in \mathcal{I}$  gathers local assignment information ( $\mathbf{W}_{i',i'}$ ,  $\mathbf{B}_{i',i'}$ ,  $\mathbf{F}_{i',i'}$ ) from its neighboring agents  $\mathcal{N}_i(t)$  within communication range (lines 4-8). Following this data aggregation, agent  $i$  utilizes its allocation bundle  $\mathbf{W}_i$  and finalization bundle  $\mathbf{F}_i$  to determine the conflict set  $\mathcal{K}_i$ , which represents the set of agents assigned for the same selected target (line 9). Employing a greedy selection strategy, agent  $i$

**Algorithm 4** Implementation and Update the Assigned Task

---

```

1: function IMPLEMENTPHASE( $\mathbf{W}_i, \mathbf{x}_i(t), \mathbf{y}(t)$ )
2: Input:  $\mathbf{W}_i, \mathbf{x}_i(t), \mathbf{y}(t)$ 
3: Output:  $\Pi(t+1), \mathbf{x}_i(t+1), \mathbf{y}(t+1)$ 
4:    $\hat{j}_i = \mathbf{W}_{i,i}$ .
5:    $\Pi(t+1) \leftarrow \Pi(t) \cup \{(i, \hat{j}_i)\}$ .
6:    $[\mathbf{x}_i(t+1), \mathbf{y}(t+1)]$ 
     = OPTCONTROL( $\mathbf{x}_i(t), \mathbf{y}(t), T$ ).
7:   if  $(t_{e,\hat{j}_i} - t) / \tau_{\hat{j}_i}^{obs} < 1$  then
8:      $\mathbf{F}_{i,i}(t+1) = 1$ .
9:   end if
10: end function

```

---

then selects the agent providing the maximum marginal utility and updates the  $\hat{i}$ -th element of its finalized bundle  $\mathbf{F}_i$  (lines 10-11). Concurrently, agent  $i$  resets the allocation bundle  $\mathbf{W}_i$  and utility bundle  $\mathbf{B}_i$  for those agents who failed to obtain the task (lines 12-15).

**D. Phase III: Implementation and Update**

Algorithm 4 details the final phase, which involves real-time updates of the allocation policy and the states of agent  $i$  and targets. Specifically, after the completion of the communication phase, agent  $i$  utilizes an optimal control function to plan its optimal trajectory (line 6). The function OPTCONTROL( $\mathbf{x}_i(t), \mathbf{y}(t), T$ ) updates the states  $\mathbf{x}_i(t+1)$  of agent  $i$  and  $\mathbf{y}(t+1)$  of targets at the subsequent time step  $t+1$ , following the agent's dynamic model (1) and the target's dynamic model (2). Ultimately, as the iteration time step  $t$  approaches the task end time for  $\hat{j}_i$ , we cease updating the task allocation policy for  $\hat{j}_i$  (lines 7-9), to ensure the convergence of Algorithm 1.

*Remark 4:* Consistent with the prevailing literature on dynamic task allocation [11], we focus on the scenario where the number of agents  $N$  exceeds the number of targets  $M$ , i.e.,  $N \geq M$ . However, it is worth noting that our proposed DGBA remains applicable even when  $N < M$ , provided multiple iterative rounds of task allocation are allowed. After each task allocation round, the bundle of unresolved tasks is promptly updated, ensuring the system's continued responsiveness and adaptability to evolving operational demands.

In summary, the proposed DGBA incorporates a greedy-based approach and negotiated consensus mechanism for distributed task allocation in the MAS. In the phase of dynamic task assignment, the algorithm employs a greedy strategy to determine the assignment that optimizes the marginal utility for each agent. Subsequently, each agent leverages the local information to construct effective task bundles. Through the constrained communication links available among them, agents engage in negotiations to arrive at a conflict-free task allocation policy. Ultimately, the DGBA executes this allocation in real time, utilizing optimal control solutions to dynamically update the states of both agents and tasks. The approximate performance of the DGBA is quantified in the subsequent section.

#### IV. PERFORMANCE GUARANTEE OF DGBA

This section presents a comprehensive performance analysis of Algorithm 1 in Problem 1. It draws upon the fundamental concepts of submodular set functions and independent systems given in Appendix A. The proofs for all lemmas and theorems are systematically presented in Appendix C.

##### A. Performance Analysis of DGBA

We designate the time step  $T$  as the moment when the final task allocation is finalized, with the corresponding final policy determined by Algorithm 1 denoted as  $\hat{\Pi} = \Pi(T)$ . As depicted in line 9 of Algorithm 2,  $\hat{j}_i$  is defined as the target selected by agent  $i$  under the allocation policy  $\hat{\Pi}$ , such that  $\hat{\Pi} = \bigcup_{i \in \mathcal{I}} \{(i, \hat{j}_i)\}$ . The marginal utility at time step  $t + 1$  is defined as  $\delta_{t+1}(\Pi(t)) = \mathcal{O}(\Pi(t+1)) - \mathcal{O}(\Pi(t))$ ,  $\forall t \in \{0, 1, \dots, T-1\}$ , and the marginal utility for element  $\pi$  is articulated as  $\delta_\pi(\Pi) = \mathcal{O}(\Pi \cup \{\pi\}) - \mathcal{O}(\Pi)$ . Let  $\Pi^*$  represent the optimal allocation for Problem 1, with the initial policy  $\Pi(0) = \emptyset$ . We define the set  $\Delta\mathcal{I}(t+1)$  as the collection of agents that update their decisions at time step  $t+1$ , given by  $\Delta\mathcal{I}(t+1) = \{i \mid \exists j \in \mathcal{J}_i(t+1), s.t. (i, j) \in \Pi(t+1) \setminus \Pi(t)\}$ .

We first provide the following lemma to characterize the properties of the sequence of agent selection sets  $\Delta\mathcal{I}(t+1)$ ,  $t \in \{0, 1, \dots, T-1\}$ .

*Lemma 1:* For the sequence of sets  $\Delta\mathcal{I}(t+1)$ , for  $t \in \{0, 1, \dots, T-1\}$ , the following properties hold:

- 1) For all distinct time steps  $t \neq t' \in \{0, 1, \dots, T-1\}$ , we have  $\Delta\mathcal{I}(t+1) \cap \Delta\mathcal{I}(t'+1) = \emptyset$ .
- 2) The union of all sets  $\Delta\mathcal{I}(t+1)$  across the entire considered time interval  $\{0, 1, \dots, T-1\}$  constitutes the complete agent set, i.e.,  $\bigcup_{t=0}^{T-1} \Delta\mathcal{I}(t+1) = \mathcal{I}$ .
- 3) The total marginal utility at time step  $t+1$  is  $\delta_{t+1}(\Pi(t)) = \sum_{i \in \Delta\mathcal{I}(t+1)} \delta_{(i, \hat{j}_i)}(\Pi(t))$ .

Building upon Lemma 1, we derive two performance bounds of the proposed DGBA for addressing Problem 1. The first bound is established through the following lemma, which provides an inequality for general normalized, non-decreasing submodular functions.

*Lemma 2:* Let  $\Omega$  be a finite ground set and  $\mathcal{O}(\cdot) : 2^\Omega \rightarrow \mathbb{R}_+$  be a normalized, non-decreasing submodular function. For any sets  $\bar{\Pi}, \tilde{\Pi} \subseteq \Omega$ , and a positive integer  $m = |\tilde{\Pi} \setminus \bar{\Pi}|$ , the following inequality holds:  $\mathcal{O}(\bar{\Pi} \cup \tilde{\Pi}) \leq \mathcal{O}(\bar{\Pi}) + \sum_{\pi \in \tilde{\Pi} \setminus \bar{\Pi}} \delta_\pi(\bar{\Pi})$ .

With Lemma 1 and Lemma 2 established, we now move forward to demonstrate the lower bound on the efficiency ratio of the DGBA for Problem 1.

*Theorem 1: (Performance Bound of DGBA).* The efficiency ratio of DGBA in Problem 1 is lower bounded by  $\frac{1}{2}$ , i.e.,  $\mathcal{O}(\hat{\Pi}) \geq \frac{1}{2} \mathcal{O}(\Pi^*)$ .

Further to the performance analysis, considering the elemental curvature  $\kappa_e$  and the properties of  $q$ -independent systems outlined in Appendix A, we present a tightness performance bound for Problem 1. We first introduce Lemma 3:

*Lemma 3:* For any finite ground set  $\Omega$  and any  $\bar{\Pi}, \tilde{\Pi} \subseteq \Omega$ , with  $m = |\tilde{\Pi} \setminus \bar{\Pi}|$ , the subsequent properties are observed:

- 1)  $\mathcal{O}(\bar{\Pi} \cup \tilde{\Pi}) \leq \mathcal{O}(\bar{\Pi}) + \xi(m) \sum_{\pi \in \tilde{\Pi} \setminus \bar{\Pi}} \delta_\pi(\bar{\Pi})$ , where  $\xi(m)$

is defined as:

$$\xi(m) = \begin{cases} \frac{1 - \kappa_e^m}{m(1 - \kappa_e)}, & 0 \leq \kappa_e < 1 \\ 1, & \kappa_e = 1 \end{cases} \quad (5)$$

In particular,  $\xi(m)$  is non-increasing with respect to  $m$  when  $0 \leq \kappa_e < 1$ , for  $m \in \mathbb{Z}_+$ .

- 2) For any  $\pi \in \tilde{\Pi} \setminus \bar{\Pi}$ , the marginal utility of the element  $\pi$  satisfies:  $\delta_\pi(\bar{\Pi}) \geq \frac{1}{\kappa_e^m} \delta_\pi(\tilde{\Pi})$ .

*Remark 5:* Based on Lemma 3, we establish that  $\mathcal{O}(\hat{\Pi} \cup \Pi^*) \leq \mathcal{O}(\hat{\Pi}) + \xi(m) \sum_{\pi \in \Pi^* \setminus \hat{\Pi}} \delta_\pi(\hat{\Pi})$ , where  $\hat{\Pi}, \Pi^* \subseteq \Omega$  and  $m = |\Pi^* \setminus \hat{\Pi}|$ . Furthermore, Lemma 3 is applicable to any submodular set functions, thereby implying  $\delta_{(i,j)}(\hat{\Pi}) \leq \kappa_e^{T-t} \delta_{(i,j)}(\Pi(t))$ ,  $\forall (i, j) \in \hat{\Pi} \setminus \Pi(t)$ .

Based on Lemma 1, Lemma 3 and Remark 5, we are now ready to establish Theorem 2 of Problem 1.

*Theorem 2: (Tightness Performance Bound of DGBA with Elemental Curvature  $\kappa_e$ ).* Given a  $q$ -independent system  $(\Omega, \mathcal{S}_q)$ , the efficiency ratio of DGBA in Problem 1 is lower bounded by  $\frac{1}{1 + \kappa_e}$ , i.e.,  $\mathcal{O}(\hat{\Pi}) \geq \frac{1}{1 + \kappa_e} \mathcal{O}(\Pi^*)$ .

*Remark 6:* Given that  $0 \leq \kappa_e \leq 1$ , it follows that  $\frac{1}{1 + \kappa_e} \geq \frac{1}{2}$ . Thus, the efficiency ratio of our proposed DGBA is at least  $\frac{1}{2}$  in the worst-case scenario.

##### B. Computational Complexity Analysis of DGBA

Furthermore, we provide an analysis of the time and space complexities of Algorithm 1.

*Theorem 3: (Complexity Analysis of DGBA).* The complexity analysis of DGBA reveals the following time and space complexities:

- The time complexity is  $O(N^2 + NM)$ .
- The space complexity is  $O(N^2 + M)$ .

Here,  $N$  represents the number of agents,  $M$  is the number of targets, and  $T$  denotes the number of time steps.

*Remark 7:* Algorithm 1 is an auction-based greedy method that offers advantages in space complexity over CBBA [18] and DGA [25]. This advantage stems from the fact that the size of data structures for the proposed DGBA scales with the number of agents rather than the number of targets. Specifically, when CBBA is applied to our problem, the space complexity is  $O(NM)$ . In scenarios where the task count may substantially outnumber the agents, such as in persistent surveillance [39] or active information gathering [40], the space complexity of CBBA increases with the number of tasks and auction frequency, potentially requiring more storage space per agent. In contrast, the DGA's data structure scales with both the number of agents and targets, leading to a space complexity of  $O(NM + N^2)$ . Additionally, DGA selects some predefined lexicographical order (which may require centralized planning or random decisions) during the conflict resolution phase to ensure a conflict-free scheme among agents. However, our proposed DGBA achieves a conflict-free task allocation policy through local information and limited communication.

#### V. APPLICATIONS AND SIMULATIONS

In this section, we focus on evaluating the performance of the proposed DGBA for cooperative task allocation in observation operations within resource-constrained micro-satellite

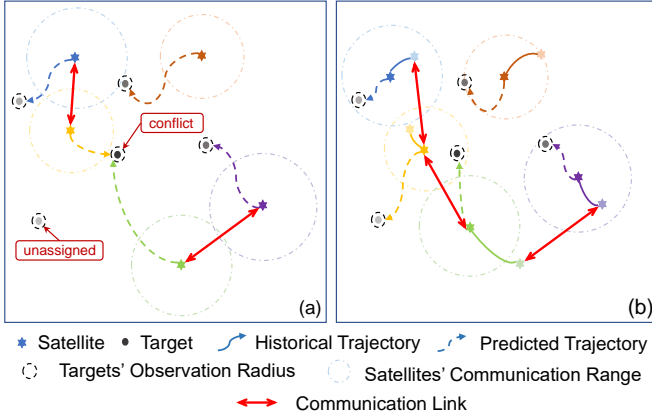


Fig. 1: *Active Observation Information Acquisition*: This scenario involves 5 mobile satellites assigned to observe 5 targets dispersed randomly within the environment. Due to the limited communication constraint, each satellite can only interact with neighboring satellites. Targets with different shades of gray represent varying levels of information value. At each time step, each satellite evaluates the objective function and marginal utility based on its current knowledge of the targets' states and selects the target that offers the maximum marginal utility for observation. The limited communication range can lead to multiple satellites selecting the same target during the task assignment phase (Fig. 1a). To achieve conflict-free task allocation, each satellite continuously updates the information within its task bundles. Additionally, their motion trajectories are incessantly replanned using the optimal control model (Fig. 1b).

constellations. The objective is to enable effective collaboration among satellites to efficiently execute multi-target observation tasks, thereby improving the overall performance of the satellite constellation. Computational simulations are performed using MATLAB R2022b on a laptop featuring an Intel Core i9 processor.

### A. Active Observation Information Acquisition

In the context of active observation information acquisition, each satellite is equipped with GPS sensors to measure the states of targets, which carry onboard instruments for observation tasks, as depicted in Fig. 1.

1) *Problem Description and Formulation*: We utilize the Earth-Centered Inertial Frame (ECI) to describe the spatial coordinates of satellites and targets. The micro-satellite constellation operates in a three-dimensional environment, starting from randomly designated initial positions. The state of satellite  $i \in \mathcal{I}$  is characterized by  $\mathbf{x}_i(t) = [\mathbf{p}_i(t), \mathbf{v}_i(t)]^\top \in \mathbb{R}^6$ , where  $\mathbf{p}_i(t) = [x_i, y_i, z_i]^\top \in \mathbb{R}^3$  is the position and  $\mathbf{v}_i(t) = [v_{ix}, v_{iy}, v_{iz}]^\top \in \mathbb{R}^3$  is the velocity of satellite  $i$ . Each satellite has the capability to control its thrust acceleration  $\mathbf{u}_i = [u_{ix}, u_{iy}, u_{iz}]^\top \in \mathbb{R}^3$  along  $x$ -,  $y$ -,  $z$ -axis, respectively. Furthermore, the state of the observed target  $j$  is defined as  $\mathbf{y}_j(t) = [\mathbf{q}_j(t), \mathbf{w}_j(t)]^\top \in \mathbb{R}^6$ , where  $\mathbf{q}_j(t)$  denotes the position and  $\mathbf{w}_j(t)$  denotes the velocity. Each agent  $i \in \mathcal{I}$  operates within a finite communication range, articulated as  $R_i^c = \phi_i L$ , where  $\phi_i$  represents the communication capability factor of agent  $i$ ,  $L$  denotes the diameter of the finite spatial domain, and  $a_{ii'}(t) > 0$  if  $\|\mathbf{p}_i(t) - \mathbf{p}_{i'}(t)\| \leq R_i^c, \forall i \neq i' \in \mathcal{I}$ .

Each satellite is tasked with reaching a circular area of a radius  $\tilde{R}_j$  around its assigned target  $j$  before the final deadline  $t_{f,j} = t_{e,j} - \tau_j^{obs}$ . The satellite then loiters around target  $j$  until the end time  $t = t_{e,j}$ , where  $\tau_j^{obs}$  indicates the anticipated observation duration of target  $j$ . The terminal constraint for information acquisition is defined as  $\Psi_i(\mathbf{p}_i(t_{f,j}), \mathbf{q}_j(t_{f,j})) = \|\mathbf{p}_i(t_{f,j}) - \mathbf{q}_j(t_{f,j})\| - \tilde{R}_j$ . Additionally, the state of target  $j$  within the time interval  $[0, t_{f,j}]$  is referred to as the maneuvering state. After time  $t_{f,j}$ , target  $j$  is assumed to be in a relatively stationary posture for the assigned satellite  $i$ . Consequently, satellite  $i$  transitions into an observation state upon satisfying the condition  $\Phi_i(t) = (t_{f,j_i} - t) / \tau_{j_i}^{obs} \leq 1$ , where  $j_i$  denotes the target assigned to satellite  $i$  at time step  $t$ .

A binary decision variable  $z_{(i,j)} \in \{0, 1\}$  is introduced for every element  $(i, j)$  to determine the assignment status. Specifically,  $z_{(i,j)} = 1$  signifies that target  $j$  is allocated to satellite  $i$ ; otherwise,  $z_{(i,j)} = 0$ . The task allocation policy is represented by the matrix  $Z = \{z_{(i,j)} \mid \forall i \in \mathcal{I}, \forall j \in \mathcal{J}\}$ . To address uncertainties in task execution, such as sensor failures or incomplete observations due to low-light conditions, a survival probability model under uncertain risk is integrated [41]. The satellites coordinate their decisions to maximize an observation utility function, denoted by  $\mathcal{Q}(Z(t))$ :

$$\mathcal{Q}(Z(t)) = \sum_{j=1}^M \mathcal{Q}_j(Z(t)), \quad (6)$$

where  $\mathcal{Q}_j(Z(t))$  signifies the observation utility of target  $j$ .

The observation utility of target  $j$  is quantified by the information value  $\rho_j$  that can be obtained within an uncertain environment:

$$\mathcal{Q}_j(Z(t)) = \rho_j \left[ 1 - \prod_{i \in \mathcal{I}} (1 - \mathcal{P}_{(i,j)}(t) z_{(i,j)}(t)) \right], \quad (7)$$

where  $\rho_j \in \mathbb{Z}_+$  signifies the information value of target  $j$ , with a higher value indicating a higher priority.  $\mathcal{P}_{(i,j)}(t) \in (0, 1)$  denotes the survival probability when satellite  $i$  approaches target  $j$  under uncertain risk, modeled as a function of the Euclidean distance  $d_{(i,j)}(t) = \|\mathbf{p}_i(t) - \mathbf{q}_j(t)\|$  between satellite  $i$  and target  $j$  at time step  $t$  [26]:

$$\mathcal{P}_{(i,j)}(t) = e^{-\lambda_j \|\mathbf{p}_i(t) - \mathbf{q}_j(t)\|}, \quad (8)$$

where  $\lambda_j \in \mathbb{Z}_+$  represents the observation decay factor. The term  $\mathcal{P}_{(i,j)}(t) z_{(i,j)}(t)$  indicates the expected probability that satellite  $i$  will successfully observe target  $j$ , and  $1 - \prod_{i \in \mathcal{I}} (1 - \mathcal{P}_{(i,j)}(t) z_{(i,j)}(t))$  denotes the joint completion probability that target  $j$  is observed by the accessible satellites. This function (7) is designed to enhance the likelihood of successfully observing target  $j$ .

Additionally, each satellite  $i \in \mathcal{I}$  is equipped with a finite fuel capacity, denoted by  $E_i$ . The cost required for satellite  $i$  to accomplish target  $j$  is represented by [19]:

$$\mathcal{C}_{(i,j)}(\mathbf{u}_i(t), \mathbf{x}_i(0), \mathbf{y}_j(t_{e,j})) = \int_0^{t_{e,j}} \mathcal{L}_i(\mathbf{x}_i(t), \mathbf{u}_i(t)) dt, \quad (9)$$

where the function  $\mathcal{L}_i(\cdot)$  accounts for the resources consumed

over the time interval  $[0, t]$  and the estimated resources that will be consumed over the time interval  $[t, t_{e,j}]$ . Given the on-board resource constraints, each satellite  $i \in \mathcal{I}$  is constrained by  $\sum_{j=1}^M \mathcal{C}_{(i,j)}(\mathbf{u}_i(t), \mathbf{x}_i(0), \mathbf{y}_j(t_{e,j}))z_{(i,j)}(t) \leq E_i$ .

A conflict-free allocation is characterized by each satellite  $i \in \mathcal{I}$  being allocated to no more than one task at any time step  $t$ , which is mathematically expressed as:

$$\sum_{j=1}^M z_{(i,j)}(t) \leq 1, \forall i \in \mathcal{I}. \quad (10)$$

The task allocation is considered complete once all satellites have transitioned into the observation state within the defined interval  $[t_{f,j}, t_{e,j}]$ .

**2) An INP Observation Task Allocation Problem:** We comprehensively consider the costs associated with satellite movement and optimize the control inputs of mobile satellites based on a task allocation policy. An optimal control input model is employed to estimate the cost incurred during satellite maneuvering. This approach enables satellites to navigate toward their designated targets, recalculating and updating their optimal task allocation in real time until all observation tasks are completed. The objective is to achieve a conflict-free allocation that correlates with the optimal control problem, thereby maximizing the global observation utility  $\mathcal{Q}(Z(t))$  for given sets of  $N$  satellites and  $M$  targets, while accounting for the risk from uncertainty. Based on the models presented in Eqs. (1), (2) and (6)-(10), this section addresses the research problem of optimal task allocation for dynamic MASs under resource constraints. The optimization problem of task allocation, incorporating real-time mobile costs, can be formulated as an INP problem:

$$\max_{Z(t)} \mathcal{Q}(Z(t)) = \sum_{j=1}^M \mathcal{Q}_j(Z(t)) \quad (11a)$$

$$s.t. \quad \sum_{j=1}^M \mathcal{C}_{(i,j)}(\mathbf{u}_i^*(t), \mathbf{x}_i(0), \mathbf{y}_j(t_{e,j}))z_{(i,j)}(t) \leq E_i, \forall i \in \mathcal{I} \quad (11b)$$

$$\sum_{j=1}^M z_{(i,j)}(t) \leq 1, \forall i \in \mathcal{I} \quad (11c)$$

$$z_{(i,j)}(t) \in \{0, 1\}, \forall i \in \mathcal{I}, \forall j \in \mathcal{J} \quad (11d)$$

where Eq. (11b) imposes the cost budget constraint, and Eq. (11c) ensures a conflict-free allocation. Moreover,  $\mathcal{C}_{(i,j)}(\mathbf{u}_i^*(t), \mathbf{x}_i(0), \mathbf{y}_j(t_{f,j}))$  is the minimum cost of maneuvering state, and  $\mathbf{u}_i^*(\cdot) : [0, t_{f,j}] \rightarrow \mathbf{U}_i(t)$  denotes the optimal control input satisfying the dynamic constraints (1)-(2).

**Proposition 1:** The dynamic task allocation problem, as formulated by the INP problem in Eqs. (11a)-(11d), is NP-hard.

**Remark 8:** The NP-hardness of the optimal task allocation problem can be demonstrated through its reduction to the classical 0-1 Knapsack Problem. By mapping the decision variable  $z_{(i,j)}(t)$ , objective function in Eq (11a), and constraints outlined in Eqs. (11b)-(11d) to their counterparts in the 0-1 Knapsack Problem, we illustrate that the dynamic

task allocation problem can be transformed into an NP-hard instance, thereby confirming its NP-hardness.

**Remark 9:** Our global utility function  $\mathcal{Q}(Z(t))$  is similar to the approach described in [42], where the cost of allocation is not explicitly incorporated. Instead, it is accounted for within the budget constraints.

**3) Problem Transformation:** According to Proposition 1, the original INP problem, as articulated in (11a)-(11d), is NP-hard. To manage this computational complexity, we reformulate it as a submodular maximization problem under a  $q$ -independent constraint, in line with Problem 1, and propose a suboptimal solution. Consider the disjoint sets  $\Omega_1, \Omega_2, \dots, \Omega_n$ , where  $\bigcup_{i=1}^N \Omega_i = \Omega$ , and  $\Omega_i \cap \Omega_{i'} = \emptyset$  for  $i \neq i'$ . For a given task allocation policy  $\Pi(t) \subseteq \Omega$ , it follows from Eq. (11c) that  $|\Pi(t) \cap \Omega_i| \leq 1$ , ensuring that each agent is allocated to at most one task. The objective function  $\mathcal{O}(\Pi(t)) = \mathcal{Q}(Z(t))$  and its components  $\mathcal{O}_j(\Pi(t)) = \mathcal{Q}_j(Z(t))$  quantify the global utility and the utility of each task, respectively. Consequently, the INP problem is reformulated as follows:

**Problem 2:**

$$\max_{\Pi(t) \subseteq \Omega} \mathcal{O}(\Pi(t)) = \sum_{j=1}^M \mathcal{O}_j(\Pi(t)) \quad (12a)$$

$$s.t. \quad \sum_{j \in \mathcal{J}_i(\Pi(t))} \mathcal{C}_{(i,j)}(\mathbf{u}_i^*(t), \mathbf{x}_i(0), \mathbf{y}_j(t_{e,j})) \leq E_i, \forall i \in \mathcal{I} \quad (12b)$$

$$|\Pi(t) \cap \Omega_i| \leq 1, \forall i \in \mathcal{I} \quad (12c)$$

Here, constraints (12b) and (12c) constitute a  $q$ -independent system, with detailed proofs provided of Lemma 4 in Appendix B and Appendix C.

Furthermore, the total cost of target  $j$  under the allocation policy  $\Pi(t)$  is expressed by:

$$\begin{aligned} \mathcal{C}_j^{tot}(\Pi(t), \mathbf{x}_i(0), \mathbf{y}_j(t_{f,j})) \\ = \sum_{i \in \mathcal{I}_j(\Pi(t))} \mathcal{C}_{(i,j)}(\mathbf{u}_i^*(t), \mathbf{x}_i(0), \mathbf{y}_j(t_{f,j})). \end{aligned}$$

**Remark 10:** In this study, the resource constraints for dynamic task allocation are primarily characterized by the motion costs of satellites, as detailed in Eq. (9), and the communication limitations among them, as specified in Assumption 1.

**Remark 11:** The detailed performance analysis of DGBA in Problem 2 in Appendix B and Appendix C. Specifically, We begin by verifying that the utility functions  $\mathcal{O}(\Pi(t))$  and  $\mathcal{O}_j(\Pi(t))$  are normalized, non-decreasing, and submodular. Furthermore, constraints (12b) and (12c) form a  $q$ -independent system. Consequently, Problem 2 can be characterized by a submodular maximization problem under a  $q$ -independent system constraint. When employing DGBA to tackle Problem 2, it is capable of obtaining an approximate solution with an efficiency ratio of  $\frac{1}{1+\kappa_e}$  within a polynomial time complexity of  $O(N^2 + NM)$ . In particular, we derive a more specific performance lower bound of  $\frac{1}{1+\kappa_e \xi((1-\frac{1}{q})N)}$  based on the settings defined in Problem 2.

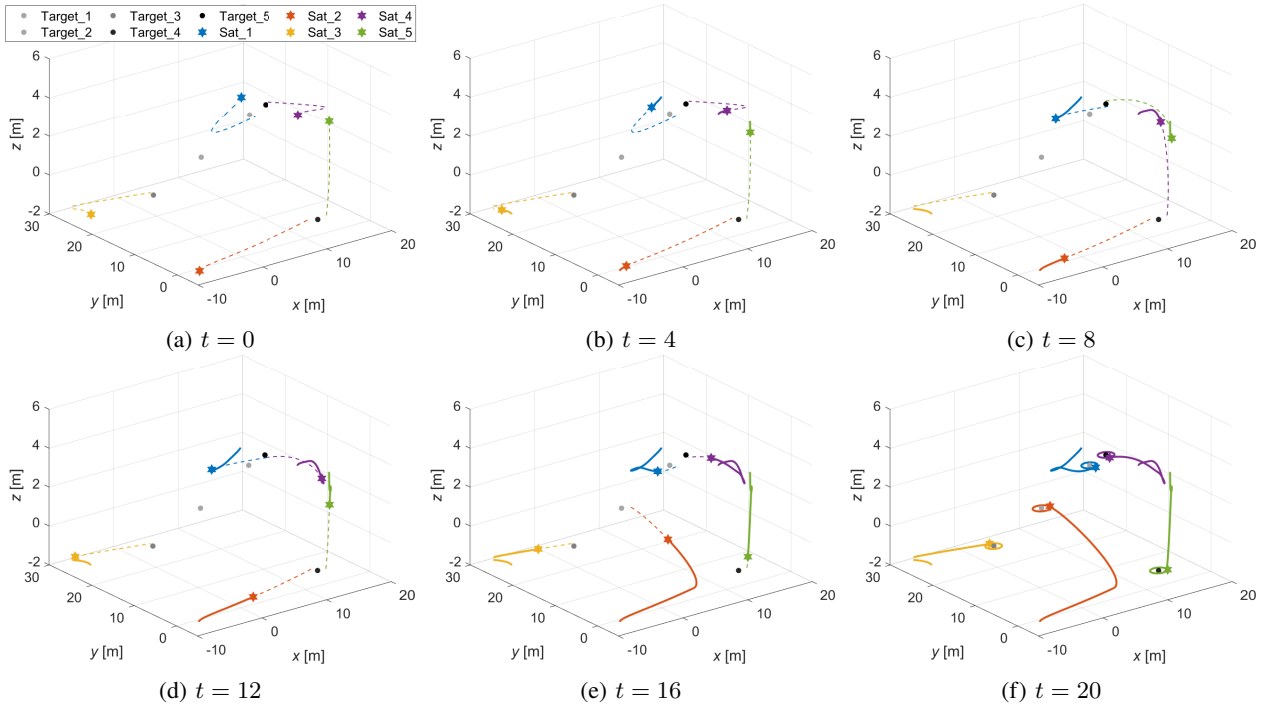


Fig. 2: *Application Simulation for Active Observation Information Acquisition*: The proposed DGBA facilitates dynamic task allocation among 5 satellites, each conducting an independent observation task, and the parameters are set as  $\phi_i = 0.3$  and  $\lambda = 0.8$ . Targets with different shades of gray represent varying levels of information value. Given the limited communication range of each satellite ( $\phi_i = 0.3$ ), a target is selected for observation, leveraging limited communication and local information. Each satellite actively approaches its assigned target, continuously updating its state and exchanging real-time information to dynamically optimize its trajectory.

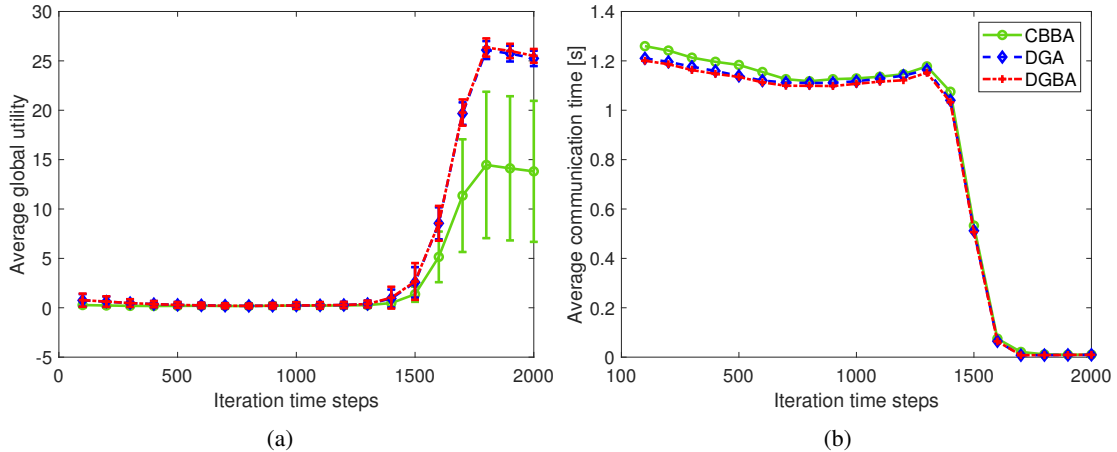


Fig. 3: Performance comparison of CBBA, DGA, and DGBA in terms of global utility and communication time over iterative time steps, with parameters set to  $\phi_i = 0.3$  and  $\lambda = 0.8$ . This figure presents a scenario where 6 satellites are tasked with observing 6 targets in real-time. To mitigate the stochastic nature of the simulations, the results are derived from the mean of ten Monte Carlo simulations, with each simulation averaging over 100 instances both preceding and succeeding each time step. The average global utility at each time step is illustrated in Fig. 3a, used to optimize the multi-agent allocation policy. Moreover, the communication time among satellites at each time step is quantified in Fig. 3b, depicting communication negotiation to achieve a conflict-free allocation.

## B. Simulated Example

This section presents numerical simulations designed to illustrate the effectiveness of Algorithm 1.

1) *Simulated Setup*: We consider a system of satellites with double integrator dynamics, and the performance index is defined as the control effort  $\mathcal{C}_{(i,j)}(\mathbf{u}_i(t), \mathbf{x}_i(0), \mathbf{y}_j(t_{e,j})) = \frac{1}{2} \int_0^{t_{e,j}} \|\mathbf{u}_i(t)\|^2 dt$ . The terminal constraint involves solving an optimal control problem with non-zero initial and terminal

velocities. The optimal control input is determined using [43]:

$$\begin{aligned} \mathbf{u}_i^*(t, t_{f,j}, \mathbf{x}_i(0), \mathbf{y}_j(t_{f,j})) &= \frac{4}{t_{f,j} - t} [\hat{\mathbf{v}}_i(t) - \mathbf{v}_i(t)] \\ &+ \frac{6}{(t_{f,j} - t)^2} [\hat{\mathbf{r}}_i(t) - \mathbf{p}_i(t) - \hat{\mathbf{v}}_i(t)(t_{f,j} - t)], \end{aligned} \quad (13)$$

where  $\hat{\mathbf{r}}_i(t) \in \mathbb{R}^3$  and  $\hat{\mathbf{v}}_i(t) \in \mathbb{R}^3$  represent the optimal position and velocity for satellite  $i$  to perform the observation

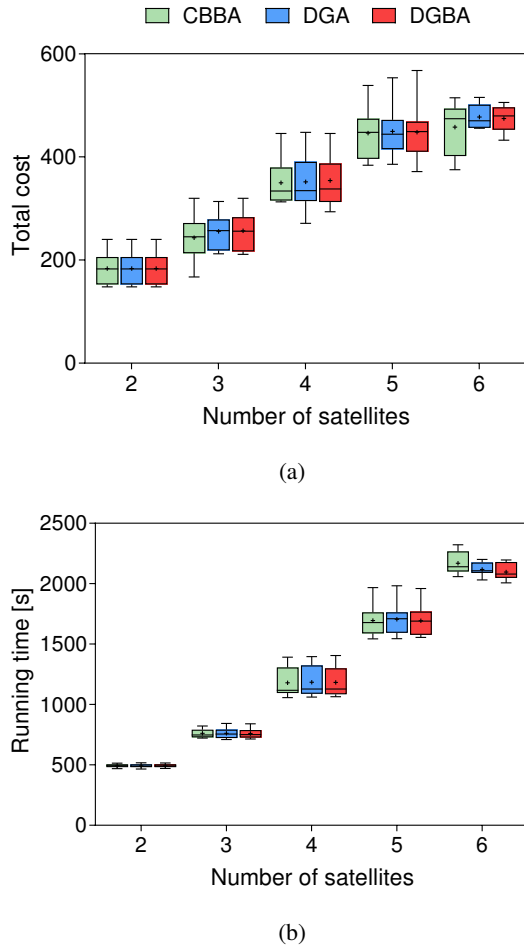


Fig. 4: Performance comparison of CBBA, DGA, and DGBA in terms of total cost and running time for different numbers of satellites, with parameters set to  $\phi_i = 0.3$  and  $\lambda = 0.8$ . The figure summarizes the statistical results from ten Monte Carlo simulations, each simulating real-time observations of random spatial targets by satellite constellations. The comparative analysis of total cost and running time for each algorithm is presented in Fig. 4a and Fig. 4b, taking into account the varying number of satellites involved.

task at the initial observation state, respectively. Eq. (13) represents a second-order differential equation with time-varying coefficients, which is numerically integrated using MATLAB’s ODE45 solver [19]. The expected end observation time for target  $j$  is set within  $t_{e,j} \in [19, 20]$  and discretized into  $T = 2000$  time steps with a constant step size  $\sigma_t = t_{e,j}/T$ . In the observation state, target  $j$  remains relative static posture for the assigned satellite  $i$ , and the satellite  $i$  calculates its centripetal acceleration  $\mathbf{u}_i^a(t)$  based on its current position  $\mathbf{p}_i(t)$ , the target  $j$ ’s position  $\mathbf{q}_j(t_{f,j})$ , and the observation radius  $\tilde{R}_j \in [1, 1.15]$  for target  $j$ . The satellite then maintains its state in orbit around target  $j$  for an observation duration  $\tau_j^{obs} \in [2, 2.5]$ . Upon completion of the observation, the satellite receives the information value  $\rho_j \in [2, 2.5]$ , where the value is positively correlated with the observation duration. The observing decay factor is set to  $\lambda_j = 0.8, \forall j \in \mathcal{J}$ . Considering the constraints imposed by onboard battery power and measurement-processing bandwidth, each satellite is restricted

to observing at most one target.

2) *Simulated Results*: We perform a dynamic task allocation, which is visually represented on a dynamic allocation map. The trajectories of the satellites subject to communication constraints, are illustrated in Fig. 2. Here, the communication range for each satellite is constrained to  $\phi_i = 0.3$ . As depicted in Fig. 2, multiple satellites are assigned to observe the same target due to limited communication and local information (as observed in Figs. 2a and 2b, satellites 2 and 5 are simultaneously assigned near target 4; in Figs. 2c and 2d, satellites 1 and 5 are simultaneously assigned near target 5, while satellites 2 and 4 are simultaneously assigned near target 4). As satellites move closer and establish communication, they exchange information, leading to task allocation and trajectory planning in real-time, thus, establishing a feasible conflict-free task allocation policy (as shown in Figs. 2e and 2f).

3) *Technical Comparison*: We conduct ten Monte Carlo simulations and average the simulation data to reduce random errors. This study presents a comprehensive performance evaluation of our proposed DGBA, benchmarking it against established methods such as CBBA [18] and DGA [25]. The comparative analysis, depicted in Fig. 3, focuses on two critical performance metrics: the average global utility and the average communication time. Analysis of Fig. 3a indicates that the average global utility of DGBA surpasses that of CBBA and DGA at each time step, which promotes satellites to find superior task allocation policies. CBBA’s performance is only approximately 60% that of DGBA at the terminal phase of task allocation. DGBA also demonstrates a lower average communication time per iteration compared to DGA and CBBA, with an initial stage time saving of 0.05 seconds in task planning, as detailed in Fig. 3b. It is a fact that CBBA employs more complex communication protocols. Furthermore, the impact of the number of satellites on task allocation efficiency is analyzed, as shown in Fig. 4. When the number of satellites and targets is less, three algorithms exhibit minimal differences in cost consumption and running time. However, as the numbers of satellites and targets increase, our proposed DGBA is capable of identifying task allocation policies with comparable cost efficiency to DGA (see Fig. 4a), but with a faster running time (see Fig. 4b). When achieving the task allocation for 6 satellites observing 6 targets, with effective control of total cost, DGBA realizes a reduction in the overall running time by 10 seconds.

## VI. CONCLUSION

This paper proposes the DGBA, an improved approach to dynamic task allocation in MASs with resource constraints. By leveraging a submodular maximization framework under  $q$ -independent system constraints, DGBA achieves a significant balance between theoretical performance and computational efficiency. The algorithm’s adaptability and low complexity make it particularly suitable for real-time applications, as demonstrated through its application to active observation information acquisition within a micro-satellite constellation. DGBA not only outperforms existing benchmark algorithms in terms of utility, cost, communication time, and running

time but also provides a feasible solution to the NP-hard task allocation problem. Future work will aim to broaden DGBA's applicability to various MASs and integrate it with machine learning techniques to further enhance performance.

## APPENDIX

### A. Preliminaries

This section establishes the foundational concepts of submodularity, independent systems, and curvature, laying the foundation for the research of this paper. Let  $\Omega$  be a finite ground set. We define a set function  $f : 2^\Omega \rightarrow \mathbb{R}_+$ , which assigns a real value to each subset of  $\Omega$ . Here, the set function is defined over the power set of  $\Omega$ , denoted by  $2^\Omega$ .

*Definition 1 ([44]):* A set function  $f : 2^\Omega \rightarrow \mathbb{R}_+$  is characterized as a normalized, non-decreasing submodular function over a non-empty finite ground set  $\Omega$  if it satisfies the subsequent properties:

- 1) Normalization:  $f(\emptyset) = 0$ .
- 2) Monotonicity: For any  $\Pi \subseteq \Pi' \subseteq \Omega$ , the set function  $f$  satisfies  $f(\Pi) \leq f(\Pi')$ .
- 3) Submodularity: For any  $\Pi \subseteq \Pi' \subseteq \Omega$  and an element  $\pi \in \Omega \setminus \Pi'$ , the inequality  $f(\Pi \cup \{\pi\}) - f(\Pi) \geq f(\Pi' \cup \{\pi\}) - f(\Pi')$  holds.

A submodular function demonstrates diminishing marginal returns. Denote  $\delta_\pi(\Pi) = f(\Pi \cup \{\pi\}) - f(\Pi)$  as the ‘‘marginal utility’’ for a given  $\Pi \subseteq \Omega$ , i.e.,  $\delta_\pi(\Pi) \geq \delta_\pi(\Pi')$ . Then, the principle of diminishing marginal returns indicates that the marginal utility gained by adding a new element to a smaller set is no less than the marginal utility gained by including it in a larger set. Another equivalent definition of submodularity is that for any subsets  $\Pi \subseteq \Omega$  and elements  $\pi \neq \pi' \in \Omega \setminus \Pi$ , one has

$$\delta_\pi(\Pi) \geq \delta_\pi(\Pi \cup \{\pi'\}). \quad (14)$$

Let  $\mathcal{S}$  denote a non-empty collection of subsets of  $\Omega$ . An independence system is defined by the pair  $(\Omega, \mathcal{S})$ , which satisfies two conditions: (a)  $\emptyset \in \mathcal{S}$ , and (b) Hereditary: For any  $\Pi' \in \mathcal{S}$ , if  $\Pi \subseteq \Pi'$ , then  $\Pi \in \mathcal{S}$ . Given an independence system  $(\Omega, \mathcal{S})$ , for any subset  $\Pi \subseteq \Omega$ , let  $\mathcal{B}(\Pi)$  denote the set of maximal independent sets in  $\Pi$ , i.e.,  $\mathcal{B}(\Pi) = \{\Pi_1 \subseteq \Pi \mid \Pi_1 \in \mathcal{S}, \forall \pi \in \Pi \setminus \Pi_1, \Pi_1 \cup \{\pi\} \notin \mathcal{S}\}$ . By the above definitions, a  $q$ -independence system can be characterized as follows:

*Definition 2: ( $q$ -Independence System [31]).* An independence system  $(\Omega, \mathcal{S}_q)$  is classified as a  $q$ -independence system if it conforms to the property of hereditary and, for any  $\Pi \subseteq \Omega$ , it satisfies

$$\max_{\Pi_1, \Pi_2 \in \mathcal{B}(\Pi)} \frac{|\Pi_1|}{|\Pi_2|} \leq q, \quad (15)$$

where  $\Pi_1, \Pi_2 \in \mathcal{S}_q$  are called the basis of  $\Pi$ .

*Definition 3: (Elemental Curvature [45]).* The elemental curvature  $\kappa_e$  of a normalized, and non-decreasing submodular function  $f : 2^\Omega \rightarrow \mathbb{R}_+$  is defined as

$$\kappa_e = \max_{\Pi \subseteq \Omega, \pi, \pi' \in \Omega \setminus \Pi, \pi \neq \pi'} \frac{\delta_\pi(\Pi \cup \{\pi'\})}{\delta_\pi(\Pi)}, \quad (16)$$

where  $\kappa_e \in [0, 1]$ .

If  $\kappa_e = 0$ , there exists a feasible set  $\Pi \in \mathcal{S}$  such that for elements  $\pi \neq \pi' \in \Omega$ , it holds that  $\delta_\pi(\Pi \cup \{\pi'\}) = 0$ . This implies that the element  $\pi$  offers no additional contribution to the function  $f$  when considering the set  $\Pi \cup \{\pi'\}$ . Conversely, if  $\kappa_e = 1$ , it indicates  $f(\Pi) = \sum_{\pi \in \Pi} f(\pi)$  for all feasible sets  $\Pi \in \mathcal{S}$ .

*Remark 12:* The elemental curvature  $\kappa_e$  can overcome the inherent and technical limitations of total curvature  $\kappa_t$ . For example,  $\kappa_t$  only provides enhanced performance bounds under conditions of weak submodularity of  $f$  over  $\Omega$  [46]. Therefore, we employ element curvature  $\kappa_e$  to investigate the tightness bound of our proposed DGBA.

### B. Performance Analysis of DGBA in Problem 2

We first prove that the global utility function  $\mathcal{O}(\Pi(t))$  and  $\mathcal{O}_j(\Pi(t))$  are normalized, non-decreasing, and submodular.

*Theorem 4:* The function  $\mathcal{O}(\Pi(t))$  is a normalized and non-decreasing submodular function.

*Remark 13 ([44]):* Since  $\mathcal{O}(\Pi(t))$  is a linear combination of the functions  $\mathcal{O}_j(\Pi(t))$ , if  $\mathcal{O}(\Pi(t))$  is normalized, non-decreasing and submodular, then each  $\mathcal{O}_j(\Pi(t))$  also inherits these properties.

Next, given the definition of  $q$ -independent systems outlined in Appendix A, we present Lemma 4 that substantiates that constraints (12b) and (12c) of Problem 2 form a  $q$ -independent system.

*Lemma 4:* The constraints (12b) and (12c) of Problem 2 constitute a  $q$ -independent system, where  $q = \lceil 1 + C_{\max}/C_{\min} \rceil$ . Here,  $C_{\max}$  and  $C_{\min}$  represent the maximum and minimum perceived costs, respectively. Specifically, these are formally defined as  $C_{\max} = \max_{\forall (i,j) \in \Omega} \mathcal{C}_{(i,j)}(\mathbf{u}_i^*(t), \mathbf{x}_i(0), \mathbf{y}_j(t_{f,j}))$  and  $C_{\min} = \min_{\forall (i,j) \in \Omega} \mathcal{C}_{(i,j)}(\mathbf{u}_i^*(t), \mathbf{x}_i(0), \mathbf{y}_j(t_{f,j}))$ .

Building upon Lemmas 1 and 4, Problem 2 is recognized as a submodular maximization problem under a  $q$ -independent system constraint. Then, we proceed to evaluate the performance of the proposed DGBA for addressing Problem 2.

*Theorem 5: (Tightness Performance Bound with  $q$ -independent System Constraint).* The efficiency ratio of DGBA in Problem 2 is lower bounded by  $\frac{1}{1 + \kappa_e \xi((1 - \frac{1}{q})N)}$ ,

i.e.,  $\mathcal{O}(\hat{\Pi}) \geq \frac{1}{1 + \kappa_e \xi((1 - \frac{1}{q})N)} \mathcal{O}(\Pi^*)$ , where

$$\xi((1 - \frac{1}{q})N) = \begin{cases} \frac{1 - \kappa_e^{(1 - \frac{1}{q})N}}{(1 - \frac{1}{q})N(1 - \kappa_e)}, & 0 \leq \kappa_e < 1 \\ 1, & \kappa_e = 1 \end{cases}$$

and  $q = \lceil 1 + C_{\max}/C_{\min} \rceil$ .

By employing the principles of submodular optimization and leveraging the properties of marginal utility, we demonstrate through problem transformation and theoretical analysis that DGBA effectively addresses Problem 2. The DGBA operates with a time complexity of  $O(N^2 + NM)$  and achieves an approximate optimal allocation with an efficiency ratio given by  $\frac{1}{1 + \kappa_e \xi((1 - \frac{1}{q})N)}$ , as established by Theorems 3 and 5.

### C. Proofs

1) *Proof of Lemma 1:* We explain each property individually:

- 1) Considering that each agent  $i \in \mathcal{I}$  is restricted to undertaking precisely one task to ensure allocation policy is conflict-free. Let  $\Delta\mathcal{I}(t)$  denote the set of agents making decisions at time step  $t$ . Since each agent can only be assigned one target, it logically follows that the sets  $\{\Delta\mathcal{I}(t+1) \mid t = 0, 1, \dots, T-1\}$  are mutually exclusive.
- 2) According to the task completion criteria outlined in Algorithm 2 (lines 14-15) and Algorithm 4 (lines 7-9), it can be inferred that all agents must have made their decisions by the algorithm's termination. Thus, we deduce that  $\bigcup_{t=0}^{T-1} \Delta\mathcal{I}(t+1) = \mathcal{I}$ .
- 3) Due to the conflict resolution in Algorithm 3 (lines 9-15), for two distinct agents  $i \neq i' \in \Delta\mathcal{I}(t+1)$ , their assignments must be different at time step  $t$ , i.e.  $\hat{j}_i \neq \hat{j}_{i'}$ . Hence, the marginal utility at time step  $t+1$  is given by:

$$\begin{aligned} \delta_{t+1}(\Pi(t)) &= \mathcal{O}(\Pi(t+1)) - \mathcal{O}(\Pi(t)) \\ &= \sum_{i \in \Delta\mathcal{I}(t+1)} \mathcal{O}_{\hat{j}_i}(\Pi(t) \cup \{(i, \hat{j}_i)\}) - \mathcal{O}_{\hat{j}_i}(\Pi(t)) \\ &= \sum_{i \in \Delta\mathcal{I}(t+1)} \delta_{(i, \hat{j}_i)}(\Pi(t)). \end{aligned}$$

2) *Proof of Lemma 2:* Let  $\tilde{\Pi} \setminus \bar{\Pi} = \{\pi_1, \pi_2, \dots, \pi_m\}$  and define  $\bar{\Pi}_t = \bar{\Pi} \cup \{\pi_1, \pi_2, \dots, \pi_t\}$  for  $t = 1, 2, \dots, m$ . Note that  $\bar{\Pi}_0 = \bar{\Pi}$  and  $\bar{\Pi}_m = \bar{\Pi} \cup (\tilde{\Pi} \setminus \bar{\Pi}) = \bar{\Pi} \cup \tilde{\Pi}$ . We then have

$$\begin{aligned} \mathcal{O}(\bar{\Pi} \cup \tilde{\Pi}) - \mathcal{O}(\bar{\Pi}) &= \mathcal{O}(\bar{\Pi}_m) - \mathcal{O}(\bar{\Pi}) \\ &= \sum_{t=0}^{m-1} (\mathcal{O}(\bar{\Pi}_{t+1}) - \mathcal{O}(\bar{\Pi}_t)) \\ &= \sum_{t=0}^{m-1} \delta_{\pi_{t+1}}(\bar{\Pi}_t) \\ &\leq \sum_{t=0}^{m-1} \delta_{\pi_{t+1}}(\bar{\Pi}), \end{aligned} \quad (17a)$$

$$= \sum_{\pi \in \tilde{\Pi} \setminus \bar{\Pi}} \delta_{\pi}(\bar{\Pi}), \quad (17b)$$

where Eq. (17a) follows from the submodularity of  $\mathcal{O}(\cdot)$  and the fact that  $\bar{\Pi} \subseteq \bar{\Pi}_t$ . Eq. (17a) is independent of the specific sequence of elements  $\pi_1, \dots, \pi_m$ , thus Eq. (17b) holds.

3) *Proof of Theorem 1:* For the optimal policy  $\Pi^*$ , each agent  $i \in \mathcal{I}$  is presumed to select a target. If an agent has not yet selected any target, we can assign a target to the agent, without diminishing the global utility. Let  $j_i^*$  denote the target assigned to agent  $i$  in the optimal policy  $\Pi^*$ . Then, we have

$$\begin{aligned} \mathcal{O}(\Pi^*) &\leq \mathcal{O}(\hat{\Pi} \cup \Pi^*) \\ &\leq \mathcal{O}(\hat{\Pi}) + \sum_{\pi \in \Pi^* \setminus \hat{\Pi}} \delta_{\pi}(\hat{\Pi}) \end{aligned} \quad (18a)$$

$$= \mathcal{O}(\hat{\Pi}) + \sum_{\substack{i \in \mathcal{I} \\ (i, j_i^*) \neq (i, \hat{j}_i)}} \delta_{(i, j_i^*)}(\hat{\Pi}) \quad (18b)$$

$$= \mathcal{O}(\hat{\Pi}) + \sum_{t=0}^{T-1} \sum_{\substack{i \in \Delta\mathcal{I}(t+1) \\ (i, j_i^*) \neq (i, \hat{j}_i)}} \delta_{(i, j_i^*)}(\hat{\Pi}) \quad (18c)$$

$$\leq \mathcal{O}(\hat{\Pi}) + \sum_{t=0}^{T-1} \sum_{\substack{i \in \Delta\mathcal{I}(t+1) \\ (i, j_i^*) \neq (i, \hat{j}_i)}} \delta_{(i, j_i^*)}(\Pi(t)) \quad (18d)$$

$$\leq \mathcal{O}(\hat{\Pi}) + \sum_{t=0}^{T-1} \sum_{\substack{i \in \Delta\mathcal{I}(t+1) \\ (i, j_i^*) \neq (i, \hat{j}_i)}} \delta_{(i, \hat{j}_i)}(\Pi(t)) \quad (18e)$$

$$= \mathcal{O}(\hat{\Pi}) + \sum_{t=0}^{T-1} \delta_{t+1}(\Pi(t)) \quad (18f)$$

$$= \mathcal{O}(\hat{\Pi}) + \mathcal{O}(\Pi(T)) - \mathcal{O}(\Pi(0)) \quad (18g)$$

$$= 2\mathcal{O}(\hat{\Pi}), \quad (18h)$$

where Eq. (18a) is obtained by Lemma 2. Eq. (18b) restates Eq. (18a) using the fact that  $\Pi^* = \bigcup_{i \in \mathcal{I}} \{(i, j_i^*)\}$ . Eq. (18c) follows from Lemma 1 1) and 2), and the fact that  $j_i^* \neq \hat{j}_i$  if  $(i, j_i^*) \notin \hat{\Pi}$ . Eq. (18d) is derived from the submodularity of  $\mathcal{O}_j(\cdot)$  and  $\Pi(t) \subseteq \hat{\Pi}$ . Eq. (18e) follows from line 9 in Algorithm 2, representing the greedy selection of a task with the maximum marginal utility. Eq. (18f) is obtained by Lemma 1. 3). Eq. (18g) is derived from definition of  $\delta_{t+1}(\Pi(t)) = \mathcal{O}(\Pi(t+1)) - \mathcal{O}(\Pi(t))$ . Eq. (18h) follows from  $\hat{\Pi} = \Pi(T)$  and  $\Pi(0) = \emptyset$ .

Thus, we conclude that  $\mathcal{O}(\hat{\Pi}) \geq \frac{1}{2}\mathcal{O}(\Pi^*)$ .

4) *Proof of Lemma 3:* Let  $\tilde{\Pi} \setminus \bar{\Pi} = \{\pi_1, \pi_2, \dots, \pi_m\}$  and define  $\bar{\Pi}_t = \bar{\Pi} \cup \{\pi_1, \pi_2, \dots, \pi_t\}$  for  $t = 1, 2, \dots, m$ . Note that  $\bar{\Pi}_0 = \bar{\Pi}$  and  $\bar{\Pi}_m = \bar{\Pi} \cup (\tilde{\Pi} \setminus \bar{\Pi}) = \bar{\Pi} \cup \tilde{\Pi}$ .

1) Firstly, we prove that Eq. (5) holds:

$$\begin{aligned} \mathcal{O}(\bar{\Pi} \cup \tilde{\Pi}) - \mathcal{O}(\bar{\Pi}) &= \mathcal{O}(\bar{\Pi}_m) - \mathcal{O}(\bar{\Pi}) \\ &= \sum_{t=0}^{m-1} (\mathcal{O}(\bar{\Pi}_{t+1}) - \mathcal{O}(\bar{\Pi}_t)) \\ &= \sum_{t=0}^{m-1} \delta_{\pi_{t+1}}(\bar{\Pi}_t). \end{aligned} \quad (19)$$

By Definition 3 of elemental curvature  $\kappa_e$ , we can derive the inequality by recursion:  $\delta_{\pi_{t+1}}(\bar{\Pi}_t) \leq \kappa_e^t \delta_{\pi_{t+1}}(\bar{\Pi})$ ,  $\forall t \in \{0, 1, \dots, m-1\}$ . Thus, Eq. (19) can be rewritten as:

$$\mathcal{O}(\bar{\Pi} \cup \tilde{\Pi}) - \mathcal{O}(\bar{\Pi}) \leq \sum_{t=0}^{m-1} \kappa_e^t \delta_{\pi_{t+1}}(\bar{\Pi}). \quad (20)$$

Given that the derived inequality (20) is independent of the specific sequence of elements  $\pi_1, \dots, \pi_m$ , we construct a set  $P$  consisting of  $m$  distinct permutations  $p$  from the entire permutation space, ensuring  $\pi_t \neq \pi'_t$  for any permutations  $p, p' \in P$  and any  $t$ . The size of set  $P$  is denoted by  $|P| = m$ . In particular, Eq. (20) holds for the  $m$  permutations in  $P$ . By summing over all such permutations in  $P$ , we obtain a comprehensive inequality that accounts for all possible orderings:

$$\begin{aligned} m(\mathcal{O}(\bar{\Pi} \cup \tilde{\Pi}) - \mathcal{O}(\bar{\Pi})) &\leq \sum_{t=0}^{m-1} \kappa_e^t \sum_{t=0}^{m-1} \delta_{\pi_{t+1}}(\bar{\Pi}) \\ &= \sum_{t=0}^{m-1} \kappa_e^t \sum_{\pi \in \tilde{\Pi} \setminus \bar{\Pi}} \delta_{\pi}(\bar{\Pi}). \end{aligned}$$

Consequently, we obtain the following:

$$\begin{aligned} & \mathcal{O}(\bar{\Pi} \cup \tilde{\Pi}) \\ & \leq \begin{cases} \mathcal{O}(\bar{\Pi}) + \frac{1-\kappa_e^m}{m(1-\kappa_e)} \sum_{\pi \in \tilde{\Pi} \setminus \bar{\Pi}} \delta_\pi(\bar{\Pi}), & 0 \leq \kappa_e < 1 \\ \mathcal{O}(\bar{\Pi}) + \sum_{\pi \in \tilde{\Pi} \setminus \bar{\Pi}} \delta_\pi(\bar{\Pi}). & \kappa_e = 1 \end{cases} \end{aligned}$$

Next, we demonstrate the monotonicity of  $\xi(m)$ . For any  $m \in \mathbb{Z}_+$  and  $0 \leq \kappa_e < 1$ , we consider the difference  $\xi(m+1) - \xi(m)$ :

$$\begin{aligned} \xi(m+1) - \xi(m) &= \frac{1 - \kappa_e^{m+1}}{(m+1)(1-\kappa_e)} - \frac{1 - \kappa_e^m}{m(1-\kappa_e)} \\ &= \frac{1 - \kappa_e^m(1+m-m\kappa_e) - 1}{1-\kappa_e} \frac{1}{m(m+1)}. \end{aligned}$$

Let  $\gamma(\kappa_e) = \kappa_e^m(1+m-m\kappa_e) - 1$ . Taking the derivative of  $\gamma(\kappa_e)$  with respect to  $\kappa_e$  yields  $\gamma'(\kappa_e) = m(m+1)(1-\kappa_e)\kappa_e^{m-1}$ . If  $0 \leq \kappa_e \leq 1$ , then  $\gamma'(\kappa_e) \geq 0$  and  $\gamma(\kappa_e)$  is non-decreasing with respect to  $\kappa_e$ . Therefore, when  $\kappa_e = 1$ ,  $\max \gamma = \gamma(1) = 0$ , then  $\gamma(\kappa_e) \leq 0$  for all  $m$ , and  $\xi(m+1) - \xi(m) \leq 0$  for  $0 \leq \kappa_e < 1$ .

2) Considering the marginal utility of adding any  $\pi \in \tilde{\Pi} \setminus \bar{\Pi}$  based on the definition of elemental curvature  $\kappa_e$  (Definition 3), we have:

$$\begin{aligned} \delta_\pi(\bar{\Pi}) &= \mathcal{O}(\bar{\Pi} \cup \{\pi\}) - \mathcal{O}(\bar{\Pi}) \\ &\geq \frac{1}{\kappa_e} (\mathcal{O}(\bar{\Pi} \cup \{\pi\} \cup \{\pi_1\}) - \mathcal{O}(\bar{\Pi} \cup \{\pi_1\})) \\ &\geq \frac{1}{\kappa_e^m} (\mathcal{O}(\bar{\Pi} \cup \{\pi\} \cup \{\pi_1\} \cup \dots \cup \{\pi_m\}) \\ &\quad - \mathcal{O}(\bar{\Pi} \cup \{\pi_1\} \cup \dots \cup \{\pi_m\})) \\ &= \frac{1}{\kappa_e^m} (\mathcal{O}(\tilde{\Pi} \cup \{\pi\}) - \mathcal{O}(\tilde{\Pi})) \\ &= \frac{1}{\kappa_e^m} \delta_\pi(\tilde{\Pi}). \end{aligned}$$

5) *Proof of Theorem 2:* For the optimal policy  $\Pi^*$ , let  $j_i^*$  denote the target assigned to agent  $i$  in  $\Pi^*$ . Then, we have

$$\begin{aligned} \mathcal{O}(\Pi^*) &\leq \mathcal{O}(\hat{\Pi} \cup \Pi^*) \\ &\leq \mathcal{O}(\hat{\Pi}) + \xi(m) \sum_{\pi \in \Pi^* \setminus \hat{\Pi}} \delta_\pi(\hat{\Pi}) \end{aligned} \quad (21a)$$

$$\begin{aligned} &= \mathcal{O}(\hat{\Pi}) + \xi(m) \sum_{t=0}^{T-1} \sum_{\substack{i \in \Delta \mathcal{I}(t+1) \\ (i, j_i^*) \neq (i, \hat{j}_i)}} \delta_{(i, j_i^*)}(\hat{\Pi}) \\ &\leq \mathcal{O}(\hat{\Pi}) + \xi(m) \sum_{t=0}^{T-1} \kappa_e^{T-t} \sum_{\substack{i \in \Delta \mathcal{I}(t+1) \\ (i, j_i^*) \neq (i, \hat{j}_i)}} \delta_{(i, j_i^*)}(\Pi(t)) \end{aligned} \quad (21b)$$

$$\begin{aligned} &\leq \mathcal{O}(\hat{\Pi}) + \xi(m) \sum_{t=0}^{T-1} \kappa_e^{T-t} \sum_{\substack{i \in \Delta \mathcal{I}(t+1) \\ (i, j_i^*) \neq (i, \hat{j}_i)}} \delta_{(i, \hat{j}_i)}(\Pi(t)) \\ &\leq \mathcal{O}(\hat{\Pi}) + \kappa_e \xi(1) \sum_{t=0}^{T-1} \delta_{t+1}(\Pi(t)) \\ &\leq \mathcal{O}(\hat{\Pi}) + \kappa_e \xi(1) (\mathcal{O}(\Pi(T)) - \mathcal{O}(\Pi(0))) \end{aligned} \quad (21c)$$

$$= (1 + \kappa_e) \mathcal{O}(\hat{\Pi}), \quad (21d)$$

where Eq. (21a) and Eq. (21b) follows from Lemma 3 and Remark 5. Eq. (21c) is derived from Lemma 3 1), which states that the function  $\xi(m)$  is non-increasing with respect to  $m$  if  $0 \leq \kappa_e < 1$  and  $m \in \mathbb{Z}_+$ . Thus, when  $m = 1$ ,  $\max \xi = \xi(1) = 1$ . Eq. (21d) is obtained by the facts that  $\xi(1) = 1$  and  $\Pi(T) = \hat{\Pi}$ .

Thus, we conclude that  $\mathcal{O}(\hat{\Pi}) \geq \frac{1}{1+\kappa_e} \mathcal{O}(\Pi^*)$ .

6) *Proof of Theorem 3:* To analyze the computational complexity of Algorithm 1, we examine the execution of each step over the  $T$  time steps.

- *Time Complexity Analysis:* In Algorithm 1, the time complexity for each agent is influenced by operations at each time step. For the assignment phase (Algorithm 2), each agent should compute marginal utilities for all available tasks, resulting in a time complexity of at most  $O(M)$  per agent. In Algorithm 3, agent  $i$  communicates with its neighbors at time step  $t$ , incurring a time complexity of  $O(|\mathcal{N}_i(t)|)$ . In the worst-case scenario, where each agent communicates with every other agent, the time complexity of  $O(N)$  per agent for the communication phase. The implementation and update phase (Algorithm 4) typically involves constant-time updates for each agent's current task assignment and state, hence  $O(1)$  per agent. Since there are  $N$  agents, the total time complexity for all agents is  $O(N^2 + NM)$ .

- *Space Complexity Analysis:* The space complexity of Algorithm 1 is determined by the data structures maintained by each agent and the communication network. Each agent maintains an allocation bundle ( $\mathbf{W}_i$ ), a utility bundle ( $\mathbf{B}_i$ ), and a finalization bundle ( $\mathbf{F}_i$ ), each requiring  $O(N)$  space to track the task allocations, utilities, and finalization status for all agents. Since there are  $N$  agents, the total space required for these structures is  $O(N^2)$ . Additionally, each agent requires  $O(M)$  space to store attributes for  $M$  targets. The adjacency matrix  $\mathcal{A}(t)$  demands  $O(N^2)$  space. Consequently, the overall space complexity of the proposed DGBA is  $O(N^2 + M)$ .

7) *Proof of Theorem 4:* Firstly, when  $\Pi(t) = \emptyset$ , it is evident that  $\prod_{i \in \mathcal{I}_j(\Pi(t))} (1 - \mathcal{P}_{(i,j)}(t)) = 1$ , thus  $\mathcal{O}(\emptyset) = 0$ .

Next, we establish the monotonicity of  $\mathcal{O}(\Pi(t))$ . Let  $\Pi(t)$  and  $\Pi'(t)$  denote two assignment policies such that  $\Pi(t) \subseteq \Pi'(t) \subseteq \Omega$ . For any  $j \in \mathcal{J}$  and  $t \in \{1, 2, \dots, T\}$ , since  $\Pi(t) \subseteq \Pi'(t)$  and  $0 < \mathcal{P}_{(i,j)}(t) < 1$  for all  $(i, j) \in \Omega$ , we have

$$\prod_{i \in \mathcal{I}_j(\Pi(t))} (1 - \mathcal{P}_{(i,j)}(t)) \geq \prod_{i \in \mathcal{I}_j(\Pi'(t))} (1 - \mathcal{P}_{(i,j)}(t)). \quad (22)$$

By subtracting  $\mathcal{O}(\Pi'(t))$  from  $\mathcal{O}(\Pi(t))$ , we can derive that

$$\begin{aligned} & \mathcal{O}(\Pi(t)) - \mathcal{O}(\Pi'(t)) \\ &= \sum_{j \in \mathcal{J}} \rho_j \left[ 1 - \prod_{i \in \mathcal{I}_j(\Pi(t))} (1 - \mathcal{P}_{(i,j)}(t)) \right] \\ &\quad - \sum_{j \in \mathcal{J}} \rho_j \left[ 1 - \prod_{i \in \mathcal{I}_j(\Pi'(t))} (1 - \mathcal{P}_{(i,j)}(t)) \right] \end{aligned}$$

$$= \sum_{j \in \mathcal{J}} \rho_j \left[ \prod_{i \in \mathcal{I}_j(\Pi'(t))} (1 - \mathcal{P}_{(i,j)}(t)) \right. \\ \left. - \prod_{i \in \mathcal{I}_j(\Pi(t))} (1 - \mathcal{P}_{(i,j)}(t)) \right].$$

By employing inequality (22), we deduce that  $\mathcal{O}(\Pi(t)) - \mathcal{O}(\Pi'(t)) \leq 0$ , thereby demonstrating that  $\mathcal{O}(\Pi(t))$  is non-decreasing.

Finally, we establish the submodularity of  $\mathcal{O}(\Pi(t))$ . Let  $\mathcal{P}_\pi$  denote the probability associated with the element  $\pi$ . The utility function  $\mathcal{O}(\Pi(t) \cup \{\pi\})$  can be expressed as follows:

$$\begin{aligned} & \mathcal{O}(\Pi(t) \cup \{\pi\}) \\ &= \sum_{j \in \mathcal{J}} \rho_j \left[ 1 - \prod_{i \in \mathcal{I}_j(\Pi(t) \cup \{\pi\})} (1 - \mathcal{P}_{(i,j)}(t)) \right] \\ &= \sum_{j \in \mathcal{J}} \rho_j \left[ 1 - (1 - \mathcal{P}_\pi) \prod_{i \in \mathcal{I}_j(\Pi(t))} (1 - \mathcal{P}_{(i,j)}(t)) \right] \\ &= \sum_{j \in \mathcal{J}} \rho_j \left[ 1 - \prod_{i \in \mathcal{I}_j(\Pi(t))} (1 - \mathcal{P}_{(i,j)}(t)) \right] \\ & \quad + \sum_{j \in \mathcal{J}} \rho_j \mathcal{P}_\pi \prod_{i \in \mathcal{I}_j(\Pi(t))} (1 - \mathcal{P}_{(i,j)}(t)). \end{aligned}$$

The difference between  $\mathcal{O}(\Pi(t))$  and  $\mathcal{O}(\Pi(t) \cup \{\pi\})$  is given by

$$\begin{aligned} & \mathcal{O}(\Pi(t) \cup \{\pi\}) - \mathcal{O}(\Pi(t)) \\ &= \sum_{j \in \mathcal{J}} \rho_j \mathcal{P}_\pi \prod_{i \in \mathcal{I}_j(\Pi(t))} (1 - \mathcal{P}_{(i,j)}(t)). \quad (23) \end{aligned}$$

By analogous derivation for  $\Pi'(t)$ , we can obtain

$$\begin{aligned} & \mathcal{O}(\Pi'(t) \cup \{\pi\}) - \mathcal{O}(\Pi'(t)) \\ &= \sum_{j \in \mathcal{J}} \rho_j \mathcal{P}_\pi \prod_{i \in \mathcal{I}_j(\Pi'(t))} (1 - \mathcal{P}_{(i,j)}(t)). \quad (24) \end{aligned}$$

From the above equations (23) and (24), we can establish the difference between  $\mathcal{O}(\Pi(t) \cup \{\pi\}) - \mathcal{O}(\Pi(t))$  and  $\mathcal{O}(\Pi'(t) \cup \{\pi\}) - \mathcal{O}(\Pi'(t))$  as

$$\begin{aligned} & [\mathcal{O}(\Pi(t) \cup \{\pi\}) - \mathcal{O}(\Pi(t))] \\ & \quad - [\mathcal{O}(\Pi'(t) \cup \{\pi\}) - \mathcal{O}(\Pi'(t))] \\ &= \sum_{j \in \mathcal{J}} \rho_j \mathcal{P}_\pi \prod_{i \in \mathcal{I}_j(\Pi(t))} (1 - \mathcal{P}_{(i,j)}(t)) \\ & \quad - \sum_{j \in \mathcal{J}} \rho_j \mathcal{P}_\pi \prod_{i \in \mathcal{I}_j(\Pi'(t))} (1 - \mathcal{P}_{(i,j)}(t)). \end{aligned}$$

Using inequality (22), it follows that the difference  $[\mathcal{O}(\Pi(t) \cup \{\pi\}) - \mathcal{O}(\Pi(t))] - [\mathcal{O}(\Pi'(t) \cup \{\pi\}) - \mathcal{O}(\Pi'(t))] \geq 0$ . This satisfies the definition of submodularity (outlined as Definition 1 3)), confirming that  $\mathcal{O}(\Pi(t))$  is submodular.

Hence,  $\mathcal{O}(\Pi(t))$  is a normalized, non-decreasing submodular function.

**8) Proof of Lemma 4:** Firstly, it is observed that any subset of feasible allocations that satisfy the constraints of Problem 2 remains feasible. Thus, constraints (12b) and (12c) of Problem 2 exhibit the property of hereditary. Consider two maximal

feasible task allocation policies,  $\hat{\Pi}$  and  $\hat{\Pi}'$ . If an element  $\pi \in \hat{\Pi}' \setminus \hat{\Pi}$  is added to  $\hat{\Pi}$ , it necessitates the removal of a subset  $\hat{\Pi}$  from  $\hat{\Pi}$ , such that  $(\hat{\Pi} \setminus \hat{\Pi} \cup \{\pi\})$  satisfies the constraints (12b) and (12c). To fulfill constraint (12b), at most  $\lceil \mathcal{C}_{\max}/\mathcal{C}_{\min} \rceil$  elements need to be removed from  $\hat{\Pi}$ . Constraint (12c) requires the removal of at most one conflicting element with  $\pi$ . These operations continue until  $\hat{\Pi} = \hat{\Pi}'$ . Thus, in the worst case, the number of removals is at least  $q = \lceil 1 + \mathcal{C}_{\max}/\mathcal{C}_{\min} \rceil$  times the number of elements, i.e., the size of  $|\hat{\Pi}| = q|\hat{\Pi}'|$ . By the definition of a  $q$ -independent system (Definition 2), constraints (12b) and (12c) form a  $q$ -independent system, where  $q = \lceil 1 + \mathcal{C}_{\max}/\mathcal{C}_{\min} \rceil$ .

**9) Proof of Theorem 5:** Since each agent can only complete at most one task, we have  $|\Pi^*| = N$ , meaning each agent is assigned exactly one observation target. Drawing parallels to the proof of Theorem 2, we derive the subsequent inequalities:

$$\begin{aligned} & \mathcal{O}(\Pi^*) \leq \mathcal{O}(\hat{\Pi} \cup \Pi^*) \\ & \leq \mathcal{O}(\hat{\Pi}) + \xi(m) \sum_{\pi \in \Pi^* \setminus \hat{\Pi}} \delta_\pi(\hat{\Pi}) \\ & = \mathcal{O}(\hat{\Pi}) + \xi(m) \sum_{t=0}^{T-1} \sum_{\substack{i \in \Delta \mathcal{I}(t+1) \\ (i, j_i^*) \neq (i, \hat{j}_i)}} \delta_{(i, j_i^*)}(\hat{\Pi}) \\ & \leq \mathcal{O}(\hat{\Pi}) + \xi(m) \sum_{t=0}^{T-1} \kappa_e^{T-t} \sum_{\substack{i \in \Delta \mathcal{I}(t+1) \\ (i, j_i^*) \neq (i, \hat{j}_i)}} \delta_{(i, \hat{j}_i)}(\Pi(t)) \\ & = \mathcal{O}(\hat{\Pi}) + \kappa_e \xi \left( \left(1 - \frac{1}{q}\right) N \right) \sum_{t=0}^{T-1} \delta_{t+1}(\Pi(t)) \quad (25a) \\ & = \left(1 + \kappa_e \xi \left( \left(1 - \frac{1}{q}\right) N \right)\right) \mathcal{O}(\hat{\Pi}), \end{aligned}$$

where

$$\xi \left( \left(1 - \frac{1}{q}\right) N \right) = \begin{cases} \frac{1 - \kappa_e^{(1 - \frac{1}{q})N}}{(1 - \frac{1}{q})N(1 - \kappa_e)}, & 0 \leq \kappa_e < 1 \\ 1, & \kappa_e = 1 \end{cases}$$

and  $q = \lceil 1 + \mathcal{C}_{\max}/\mathcal{C}_{\min} \rceil$ . Eq. (25a) is derived from  $m = |\Pi^* \setminus \hat{\Pi}| = \left(1 - \frac{1}{q}\right)N$ .

Thus, we conclude that  $\mathcal{O}(\hat{\Pi}) \geq \frac{1}{1 + \kappa_e \xi \left( \left(1 - \frac{1}{q}\right) N \right)} \mathcal{O}(\Pi^*)$ .

## REFERENCES

- [1] S. C. Pinto, S. Welikala, S. B. Andersson, J. M. Hendrickx, and C. G. Cassandras, "Minimax persistent monitoring of a network system," *Automatica*, vol. 149, p. 110808, 2023.
- [2] N. Rezazadeh and S. S. Kia, "A sub-modular receding horizon solution for mobile multi-agent persistent monitoring," *Automatica*, vol. 127, p. 109460, 2021.
- [3] V. N. Hartmann, A. Orthey, D. Driess, O. S. Oguz, and M. Toussaint, "Long-horizon multi-robot rearrangement planning for construction assembly," *IEEE Transactions on Robotics*, vol. 39, no. 1, pp. 239–252, 2022.
- [4] T. Li, H.-S. Shin, and A. Tsourdos, "Threshold bundle-based task allocation for multiple aerial robots," *IFAC-PapersOnLine*, vol. 53, no. 2, pp. 14 787–14 792, 2020.

- [5] K. Chen, W. He, W. X. Zheng, W. Zhang, and Y. Tang, "Minimal leader selection in general linear multi-agent systems with switching topologies: Leveraging submodularity ratio," *IEEE Transactions on Circuits and Systems I: Regular Papers*, vol. 70, no. 4, pp. 1720–1732, 2023.
- [6] D. Paccagnan, R. Chandan, and J. R. Marden, "Utility design for distributed resource allocation—part i: Characterizing and optimizing the exact price of anarchy," *IEEE Transactions on Automatic Control*, vol. 65, no. 11, pp. 4616–4631, 2019.
- [7] A. Hashemi, M. Ghasemi, H. Vikalo, and U. Topcu, "Randomized greedy sensor selection: Leveraging weak submodularity," *IEEE Transactions on Automatic Control*, vol. 66, no. 1, pp. 199–212, 2020.
- [8] Q. Hou and A. Clark, "Robust maximization of correlated submodular functions under cardinality and matroid constraints," *IEEE Transactions on Automatic Control*, vol. 66, no. 12, pp. 6148–6155, 2021.
- [9] W. Yao, N. Qi, N. Wan, and Y. Liu, "An iterative strategy for task assignment and path planning of distributed multiple unmanned aerial vehicles," *Aerospace Science and Technology*, vol. 86, pp. 455–464, 2019.
- [10] B. Du, K. Qian, C. Claudel, and D. Sun, "Jacobi-style iteration for distributed submodular maximization," *IEEE Transactions on Automatic Control*, vol. 67, no. 9, pp. 4687–4702, 2022.
- [11] L. Zhou and P. Tokekar, "Risk-aware submodular optimization for multirobot coordination," *IEEE Transactions on Robotics*, vol. 38, no. 5, pp. 3064–3084, 2022.
- [12] A. Samiei and L. Sun, "Distributed matching-by-clone Hungarian-based algorithm for task allocation of multiagent systems," *IEEE Transactions on Robotics*, vol. 40, pp. 851–863, 2024.
- [13] C. H. Liu, X. Ma, X. Gao, and J. Tang, "Distributed energy-efficient multi-uav navigation for long-term communication coverage by deep reinforcement learning," *IEEE Transactions on Mobile Computing*, vol. 19, no. 6, pp. 1274–1285, 2019.
- [14] L. Feng, W. Zhou, W. Liu, Y.-S. Ong, and K. C. Tan, "Solving dynamic multiobjective problem via autoencoding evolutionary search," *IEEE Transactions on Cybernetics*, vol. 52, no. 5, pp. 2649–2662, 2020.
- [15] X. Jin, Y. Shi, Y. Tang, H. Werner, and J. Kurths, "Event-triggered fixed-time attitude consensus with fixed and switching topologies," *IEEE Transactions on Automatic Control*, vol. 67, no. 8, pp. 4138–4145, 2022.
- [16] Y. Wang, H. Li, and Y. Yao, "An adaptive distributed auction algorithm and its application to multi-AUV task assignment," *Science China Technological Sciences*, pp. 1–10, 2023.
- [17] J. Wang, Z. Zhou, X. Jin, S. Mao, and Y. Tang, "Matching-based capture-the-flag games for multi-agent systems," *IEEE Transactions on Cognitive and Developmental Systems*, 2023.
- [18] H.-L. Choi, L. Brunet, and J. P. How, "Consensus-based decentralized auctions for robust task allocation," *IEEE Transactions on Robotics*, vol. 25, no. 4, pp. 912–926, 2009.
- [19] M. Braquet and E. Bakolas, "Greedy decentralized auction-based task allocation for multi-agent systems," *IFAC-PapersOnLine*, vol. 54, no. 20, pp. 675–680, 2021.
- [20] I. Jang, H.-S. Shin, and A. Tsourdos, "Anonymous hedonic game for task allocation in a large-scale multiple agent system," *IEEE Transactions on Robotics*, vol. 34, no. 6, pp. 1534–1548, 2018.
- [21] E. Bakolas and Y. Lee, "Decentralized game-theoretic control for dynamic task allocation problems for multi-agent systems," in *2021 American Control Conference (ACC)*. IEEE, 2021, pp. 3228–3233.
- [22] E. Seraj, L. Chen, and M. C. Gombolay, "A hierarchical coordination framework for joint perception-action tasks in composite robot teams," *IEEE Transactions on Robotics*, vol. 38, no. 1, pp. 139–158, 2021.
- [23] M. Yang, J. Zhao, X. Hu, W. Zhou, J. Zhu, and H. Li, "LDSA: Learning dynamic subtask assignment in cooperative multi-agent reinforcement learning," *Advances in Neural Information Processing Systems*, vol. 35, pp. 1698–1710, 2022.
- [24] G. Qu, D. Brown, and N. Li, "Distributed greedy algorithm for satellite assignment problem with submodular utility function," *IFAC-PapersOnLine*, vol. 48, no. 22, pp. 258–263, 2015.
- [25] G. Qu, D. Brown, and N. Li, "Distributed greedy algorithm for multi-agent task assignment problem with submodular utility functions," *Automatica*, vol. 105, pp. 206–215, 2019.
- [26] X. Sun, C. G. Cassandras, and X. Meng, "Exploiting submodularity to quantify near-optimality in multi-agent coverage problems," *Automatica*, vol. 100, pp. 349–359, 2019.
- [27] D. Paccagnan and J. R. Marden, "Utility design for distributed resource allocation—part ii: applications to submodular, covering, and supermodular problems," *IEEE Transactions on Automatic Control*, vol. 67, no. 2, pp. 618–632, 2021.
- [28] K. Chen, W. He, Q.-L. Han, M. Xue, and Y. Tang, "Leader selection in networks under switching topologies with antagonistic interactions," *Automatica*, vol. 142, p. 110334, 2022.
- [29] N. Rezazadeh and S. S. Kia, "Distributed strategy selection: A submodular set function maximization approach," *Automatica*, vol. 153, p. 111000, 2023.
- [30] O. Shorinwa, R. N. Haksar, P. Washington, and M. Schwager, "Distributed multirobot task assignment via consensus ADMM," *IEEE Transactions on Robotics*, 2023.
- [31] D. R. Fulkerson, M. Balinski, and A. J. Hoffman, "Mathematical programming study 8 - polyhedral combinatorics-dedicated to the memory of d.r. fulkerson," *Mathematical Programming*, vol. 16, no. 1, p. 132–135, 1979.
- [32] G. L. Nemhauser, L. A. Wolsey, and M. L. Fisher, "An analysis of approximations for maximizing submodular set functions—i," *Mathematical programming*, vol. 14, pp. 265–294, 1978.
- [33] M. L. Fisher, G. L. Nemhauser, and L. A. Wolsey, *An analysis of approximations for maximizing submodular set functions—II*. Springer, 1978.
- [34] V. Tzoumas, A. Jadbabaie, and G. J. Pappas, "Robust and adaptive sequential submodular optimization," *IEEE Transactions on Automatic Control*, vol. 67, no. 1, pp. 89–104, 2022.
- [35] B. Wie, *Space vehicle dynamics and control*. AIAA, 1998.
- [36] B. R. Munson, D. F. Young, and T. H. Okiishi, "Fundamentals of fluid mechanics," *Oceanographic Literature Review*, vol. 10, no. 42, p. 831, 1995.
- [37] A. Downie, B. Ghahesifard, and S. L. Smith, "Submodular maximization with limited function access," *IEEE Transactions on Automatic Control*, 2022.
- [38] B. Fu, W. Smith, D. M. Rizzo, M. Castanier, M. Ghaffari, and K. Barton, "Robust task scheduling for heterogeneous robot teams under capability uncertainty," *IEEE Transactions on Robotics*, vol. 39, no. 2, pp. 1087–1105, 2022.
- [39] X. Jin, Y. Shi, Y. Tang, and X. Wu, "Event-triggered attitude consensus with absolute and relative attitude measurements," *Automatica*, vol. 122, p. 109245, 2020.
- [40] B. Schlotfeldt, V. Tzoumas, and G. J. Pappas, "Resilient active information acquisition with teams of robots," *IEEE Transactions on Robotics*, vol. 38, no. 1, pp. 244–261, 2021.
- [41] A. Prasad, J. Hudack, S. Mou, and S. Sundaram, "Policies for risk-aware sensor data collection by mobile agents," *Automatica*, vol. 142, p. 110391, 2022.
- [42] H. Aziz, H. Chan, Á. Cseh, B. Li, F. Ramezani, and C. Wang, "Multi-robot task allocation—complexity and approximation," *arXiv preprint arXiv:2103.12370*, 2021.
- [43] R. H. Battin, *An introduction to the mathematics and methods of astrodynamics*. AIAA, 1999.
- [44] A. Krause and D. Golovin, "Submodular function maximization," *Tractability*, vol. 3, no. 71–104, p. 3, 2014.
- [45] Z. Wang, B. Moran, X. Wang, and Q. Pan, "Approximation for maximizing monotone non-decreasing set functions with a greedy method," *Journal of Combinatorial Optimization*, vol. 31, pp. 29–43, 2016.
- [46] S. Welikala, C. G. Cassandras, H. Lin, and P. J. Antsaklis, "A new performance bound for submodular maximization problems and its application to multi-agent optimal coverage problems," *Automatica*, vol. 144, p. 110493, 2022.